

A mixed virtual element method for quasi-Newtonian Stokes flows*

ERNESTO CÁCERES[†] GABRIEL N. GATICA[‡] FILÁNDER A. SEQUEIRA[§]

Abstract

In this paper we introduce and analyze a virtual element method (VEM) for an augmented mixed variational formulation of a class of nonlinear Stokes models arising in quasi-Newtonian fluids. While the original unknowns are given by the pseudostress, the velocity, and the pressure, the latter is eliminated by using the incompressibility condition, and in order to handle the nonlinearity involved, the velocity gradient is set as an auxiliary one. In this way, and adding a redundant term arising from the constitutive equation relating the pseudostress and the velocity, an augmented formulation showing a saddle point structure is obtained, whose well-posedness has been established previously by using known results from nonlinear functional analysis. Then, following the basic principles and ideas of the mixed-VEM approach, we introduce a Galerkin scheme employing generic virtual element subspaces and projectors satisfying suitable abstract conditions, and derive the corresponding solvability analysis, along with the associated *a priori* error estimates for the virtual element solution as well as for the fully computable projection of it. Next, we provide two specific choices of subspaces and local projectors verifying the required hypotheses, one of them yielding an optimally convergent mixed-VEM for the fully nonlinear problem studied here, and the other one providing a new approach for the linear version of it, that is for the Stokes problem. In addition, we are able to apply a second element-by-element postprocessing formula for the pseudostress, which yields an optimally convergent approximation of it with respect to the broken $\mathbb{H}(\mathbf{div})$ -norm. Finally, several numerical results illustrating the good performance of the method and confirming the theoretical rates of convergence are reported.

Key words: nonlinear Stokes equations, virtual element method, a priori error analysis

Mathematics subject classifications (2000): 65N30, 65N12, 65N15, 76D07.

1 Introduction

A virtual element method (VEM) for a dual-mixed variational formulation of the Stokes problem, in which the pseudostress and the velocity are the only unknowns, whereas the pressure is computed via a postprocessing formula, was introduced and analyzed in the recent paper [12]. In fact, following the

*This work was partially supported by CONICYT-Chile through BASAL project CMM, Universidad de Chile, project Anillo ACT1118 (ANANUM), and the Becas-CONICYT Programme for foreign students; by Centro de Investigación en Ingeniería Matemática (CI²MA), Universidad de Concepción; and by Universidad Nacional (Costa Rica), through the project 0106-16.

[†]CI²MA and Departamento de Ingeniería Matemática, Universidad de Concepción, Casilla 160-C, Concepción, Chile, email: ecaceresv@udec.cl. Present address: Division of Applied Mathematics, Brown University, Providence, RI 02912, USA, email: ernesto.caceres.valenzuela@brown.edu.

[‡]CI²MA and Departamento de Ingeniería Matemática, Universidad de Concepción, Casilla 160-C, Concepción, Chile, email: ggatica@ci2ma.udec.cl.

[§]Escuela de Matemática, Universidad Nacional, Campus Omar Dengo, Heredia, Costa Rica, email: filander.sequeira@una.cr.

basic principles provided in [9], the approach in [12] firstly introduces the main ingredients of the mixed-VEM, which includes the virtual finite element subspaces to be employed, the associated interpolation operators, and the respective approximation properties. Arbitrary polygonal meshes satisfying the conditions specified in [9] are allowed for the decomposition of the computational domain. Then, bearing in mind that the main bilinear form involves terms with deviatoric tensors, and aiming to construct an explicitly calculable discrete version of it, a new local projector onto a suitable polynomial space, which takes into account the main features of the continuous solution and allows the explicit integration of the aforementioned terms, is proposed in [12]. Moreover, the uniform boundedness of the resulting family of projectors and its corresponding approximation properties are established there. In this way, and applying the classical Babuška-Brezzi theory, the well-posedness of the actual Galerkin scheme is proved and the associated *a priori* error estimates for the virtual solution as well as for the fully computable projection of it are derived.

In connection with the above, we highlight that the derivation of pseudostress-based dual-mixed finite element methods for problems in continuum mechanics has become a very active research area in the last decade, mainly because of the need of finding new ways of circumventing the symmetry requirement of the usual stress-based approach. Here we mean by *dual-mixed* those methods in which the main unknown of the resulting saddle point problem lives in either a vectorial $\mathbf{H}(\text{div})$ or a tensorial $\mathbb{H}(\mathbf{div})$ space. In particular, one of the most popular approaches is precisely the pseudostress-velocity formulation employed in [12], which after being introduced first in [14], has been furtherly developed, among others, in [22] and [23], where the latter deals with the nonlinear model determined by quasi-Newtonian Stokes flows. Further applications of pseudostress-based dual-mixed formulations to nonlinear Stokes problems can be found in [15], [21], and [25]. In turn, other applications of this approach in fluid mechanics are available for instance in [17] and [18], where dual-mixed methods for the linear and nonlinear versions of the Brinkman problem are studied.

Consequently, the increasing applicability of the aforementioned pseudostress-based approach, together with the well-known advantages of the recently introduced VEM philosophy (see, e.g. [3], [5], [6], [7], [9], and the references therein), have motivated us to combine both procedures for numerically solving boundary value problems in fluid mechanics. Indeed, besides the already described contribution [12] concerning the Stokes problem, we now refer to [13] where we have proposed two mixed virtual element methods for the two-dimensional Brinkman problem studied in [17]. More precisely, proceeding as in this latter reference, we first use the equilibrium equation and the incompressibility condition to eliminate the velocity and the pressure, respectively, thus yielding the pseudostress as the only unknown of the resulting dual-mixed formulation in [13]. Then, in order to define a calculable discrete bilinear form, whose continuous version also involves deviatoric tensors (as in [12]), we propose two different projectors: the particular local one introduced in [12], and the general L^2 -orthogonal projection analyzed in [6] (see also [7]). Next, we apply the classical Lax-Milgram Lemma to show that the resulting mixed virtual element schemes are well-posed, and derive the associated *a priori* error estimates for the virtual solutions as well as for the fully computable projections of them. In addition, following [19] and [20], we propose a second element-by-element postprocessing formula for the pseudostress, which yields an optimally convergent approximation of this unknown with respect to the broken $\mathbb{H}(\mathbf{div})$ -norm. A very interesting feature of both mixed virtual element methods proposed in [13] refers to their robustness as the Stokes limit of Brinkman is approached. For further recent contributions on virtual element methods, though not necessarily connected to the pseudostress-based approach or to dual-mixed methods, we refer to [1], [4], [8], [11], [16], and [28].

According to the foregoing discussion, and in order to continue developing mixed virtual element methods in fluid mechanics, we now aim to extend the analysis and results from [12] and [13] to the case of quasi-Newtonian Stokes flows, for which we consider the nonlinear problem studied in [23] (see also [24]) as our motivating model. The rest of this work is organized as follows. In Section 2 we introduce the boundary value problem of interest, recall from [23] its augmented pseudostress-velocity mixed

formulation, and state the corresponding well-posedness result. In turn, in Section 3 we first use generic virtual element subspaces and projectors satisfying suitable abstract conditions to define our associated Galerkin scheme. Then, we establish the unique solvability of it and derive the corresponding *a priori* error estimates for both the virtual element solution and its fully computable projection. We remark that a nonlinear version of the Babuška-Brezzi theory is required here. Next, two specific choices of subspaces and local projectors satisfying the aforementioned abstract assumptions are described in Section 4. However, we remark in advance that only one of them will lead to a fully satisfactory virtual element scheme for our fully nonlinear problem, whereas the other choice, determined by the local projector introduced in [12], will provide an alternative mixed-VEM for the linear Stokes problem. Furthermore, at the end of Section 4 we suggest a second element-by-element postprocessing formula for this variable, which yields an optimally convergent approximation of it with respect to the broken $\mathbb{H}(\mathbf{div})$ -norm. Finally, in Section 5 we present several numerical results illustrating the good performance of the method and confirming the theoretical rates of convergence.

Notations

We end the present section with several useful notations to be used below. We begin by mentioning that, given a non-null space \mathbf{H} , we set $\mathbf{H} := \mathbf{H}^2$ and $\mathbb{H} := \mathbf{H}^{2 \times 2}$. In addition, standard terminology will be adopted for Sobolev spaces $\mathbf{H}^s(\Omega)$, $s \in \mathbb{R}$, with norm $\|\cdot\|_{s,\Omega}$ and seminorm $|\cdot|_{s,\Omega}$. In particular, we usually write $L^2(\Omega)$ instead of $\mathbf{H}^0(\Omega)$. In turn, $\mathbf{H}^{1/2}(\Gamma)$ is the space of traces of functions of $\mathbf{H}^1(\Omega)$, $\mathbf{H}^{-1/2}(\Gamma)$ denotes its dual, and $\langle \cdot, \cdot \rangle_\Gamma$ stands for the duality pairing between them or between $\mathbf{H}^{-1/2}(\Gamma)$ and $\mathbf{H}^{1/2}(\Gamma)$. Then, letting \mathbf{div} be the usual divergence operator \mathbf{div} acting along the rows of a given tensor, we recall that the spaces

$$\mathbf{H}(\mathbf{div}; \Omega) := \left\{ \boldsymbol{\tau} \in \mathbf{L}^2(\Omega) : \mathbf{div}(\boldsymbol{\tau}) \in L^2(\Omega) \right\},$$

and

$$\mathbb{H}(\mathbf{div}; \Omega) := \left\{ \boldsymbol{\tau} \in \mathbb{L}^2(\Omega) : \mathbf{div}(\boldsymbol{\tau}) \in L^2(\Omega) \right\},$$

equipped with the usual norms

$$\|\boldsymbol{\tau}\|_{\mathbf{div};\Omega}^2 := \|\boldsymbol{\tau}\|_{0,\Omega}^2 + \|\mathbf{div}(\boldsymbol{\tau})\|_{0,\Omega}^2 \quad \forall \boldsymbol{\tau} \in \mathbf{H}(\mathbf{div}; \Omega),$$

and

$$\|\boldsymbol{\tau}\|_{\mathbb{div};\Omega}^2 := \|\boldsymbol{\tau}\|_{0,\Omega}^2 + \|\mathbf{div}(\boldsymbol{\tau})\|_{0,\Omega}^2 \quad \forall \boldsymbol{\tau} \in \mathbb{H}(\mathbf{div}; \Omega),$$

are Hilbert spaces. Furthermore, given $\boldsymbol{\tau} := (\tau_{ij})$, $\boldsymbol{\zeta} := (\zeta_{ij}) \in \mathbb{R}^{2 \times 2}$, we write as usual

$$\boldsymbol{\tau}^t := (\tau_{ji}), \quad \text{tr}(\boldsymbol{\tau}) := \sum_{i=1}^2 \tau_{ii}, \quad \boldsymbol{\tau}^d := \boldsymbol{\tau} - \frac{1}{2} \text{tr}(\boldsymbol{\tau}) \mathbb{I}, \quad \text{and} \quad \boldsymbol{\tau} : \boldsymbol{\zeta} := \sum_{i,j=1}^2 \tau_{ij} \zeta_{ij},$$

where \mathbb{I} is the identity matrix of $\mathbb{R}^{2 \times 2}$. Finally, in what follows we employ $\mathbf{0}$ to denote a generic null vector, null tensor or null operator, and use C , with or without subscripts, bars, tildes or hats, to denote generic constants independent of the discretization parameters, which may take different values at different places.

2 The nonlinear Stokes problem and its mixed formulation

2.1 The model problem

Given a bounded and simply connected polygonal domain Ω in \mathbb{R}^2 with boundary Γ , we are interested in determining the velocity \mathbf{u} , the pseudostress tensor $\boldsymbol{\sigma}$ and the pressure p of a quasi-Newtonian

Stokes flow occupying Ω , under the action of external forces. More precisely, given a volume force $\mathbf{f} \in \mathbf{L}^2(\Omega)$ and a Dirichlet datum $\mathbf{g} \in \mathbf{H}^{1/2}(\Gamma)$, we seek a tensor field $\boldsymbol{\sigma}$, a vector field \mathbf{u} , and a scalar field p such that

$$\begin{aligned} \boldsymbol{\sigma} &= 2\mu(|\nabla\mathbf{u}|)\nabla\mathbf{u} - p\mathbb{I} \quad \text{in } \Omega, & \mathbf{div}(\boldsymbol{\sigma}) &= -\mathbf{f} \quad \text{in } \Omega, \\ \mathbf{div}(\mathbf{u}) &= 0 \quad \text{in } \Omega, & \mathbf{u} &= \mathbf{g} \quad \text{on } \Gamma, & \int_{\Omega} p &= 0, \end{aligned} \quad (2.1)$$

where $\mu : \mathbb{R}^+ \rightarrow \mathbb{R}^+$ is the nonlinear kinematic viscosity function of the fluid, and $|\cdot|$ is the euclidean norm of $\mathbb{R}^{2 \times 2}$. As required by the incompressibility condition, we assume that \mathbf{g} satisfies the compatibility condition $\int_{\Gamma} \mathbf{g} \cdot \mathbf{n} = 0$, where \mathbf{n} stands for the unit outward normal at Γ . The kind of nonlinear Stokes problem given by (2.1) appears in the modeling of a large class of non-Newtonian fluids (see e.g. [2, 26, 27, 29]). In particular, the Ladyzhenskaya law for fluids with large stresses (see [26]), also known as power law, is given by $\mu(t) := \kappa_0 + \kappa_1 t^{\beta-2} \quad \forall t \in \mathbb{R}^+$, with $\kappa_0 \geq 0$, $\kappa_1 > 0$ and $\beta > 1$, and the Carreau law for viscoplastic flows (see e.g. [27, 29]) reads $\mu(t) := \kappa_0 + \kappa_1(1+t^2)^{(\beta-2)/2} \quad \forall t \in \mathbb{R}^+$, with $\kappa_0 \geq 0$, $\kappa_1 > 0$ and $\beta > 1$.

In what follows, we let $\mu_{ij} : \mathbb{R}^{2 \times 2} \rightarrow \mathbb{R}$ be the mapping given by $\mu_{ij}(\mathbf{r}) := \mu(|\mathbf{r}|)r_{ij}$ for each $\mathbf{r} := (r_{ij}) \in \mathbb{R}^{2 \times 2}$ and for each $i, j \in \{1, 2\}$. Then, throughout this paper we assume that μ is of class C^1 and that there exist $\gamma_0, \alpha_0 > 0$ such that for each $\mathbf{r} := (r_{ij})$, $\mathbf{s} := (s_{ij}) \in \mathbb{R}^{2 \times 2}$, there hold

$$|\mu_{ij}(\mathbf{r})| \leq \gamma_0 |\mathbf{r}|, \quad \text{and} \quad \left| \frac{\partial}{\partial r_{kl}} \mu_{ij}(\mathbf{r}) \right| \leq \gamma_0 \quad \forall i, j, k, l \in \{1, 2\}, \quad (2.2)$$

and

$$\sum_{i,j,k,l=1}^2 \frac{\partial}{\partial r_{kl}} \mu_{ij}(\mathbf{r}) s_{ij} s_{kl} \geq \alpha_0 |\mathbf{s}|^2. \quad (2.3)$$

It is easy to check that the Carreau law satisfies (2.2) and (2.3) for all $\kappa_0 > 0$ and for all $\beta \in [1, 2]$. In particular, with $\beta = 2$ we recover the usual linear Stokes model.

2.2 The continuous formulation

We now recall from [23] the augmented mixed variational formulation of (2.1). In fact, we first observe that, using the incompressibility condition (cf. third equation in (2.1)) to eliminate the pressure, and introducing the auxiliary unknown $\mathbf{t} := \nabla\mathbf{u}$ for a better handling of the nonlinearity determined by the kinematic viscosity μ , our model problem (2.1) can be rewritten equivalently as:

$$\begin{aligned} \boldsymbol{\sigma}^d &= 2\mu(|\mathbf{t}|)\mathbf{t} \quad \text{in } \Omega, & \mathbf{div}(\boldsymbol{\sigma}) &= -\mathbf{f} \quad \text{in } \Omega, \\ \mathbf{t} &= \nabla\mathbf{u} \quad \text{in } \Omega, & \mathbf{u} &= \mathbf{g} \quad \text{on } \Gamma, & \int_{\Omega} \text{tr}(\boldsymbol{\sigma}) &= 0, \end{aligned} \quad (2.4)$$

where the pressure p can be recovered by the postprocessing formula

$$p = -\frac{1}{2} \text{tr}(\boldsymbol{\sigma}). \quad (2.5)$$

Next, proceeding as explained in [23], in particular enriching the variational formulation resulting at first instance with a further testing of the constitutive law relating $\boldsymbol{\sigma}$ and \mathbf{t} (cf. first equation of (2.4)), which includes its multiplication by a stabilization parameter $\kappa > 0$ to be suitably chosen later on, we arrive at the following saddle point-type nonlinear system: Find $((\mathbf{t}, \boldsymbol{\sigma}), \mathbf{u}) \in (X \times H) \times Y$ such that

$$\begin{aligned} [\mathcal{A}(\mathbf{t}, \boldsymbol{\sigma}), (\mathbf{s}, \boldsymbol{\tau})] + [\mathcal{B}(\mathbf{s}, \boldsymbol{\tau}), \mathbf{u}] &= [\mathcal{F}, (\mathbf{s}, \boldsymbol{\tau})] \quad \forall (\mathbf{s}, \boldsymbol{\tau}) \in X \times H, \\ [\mathcal{B}(\mathbf{t}, \boldsymbol{\sigma}), \mathbf{v}] &= [\mathcal{G}, \mathbf{v}] \quad \forall \mathbf{v} \in Y, \end{aligned} \quad (2.6)$$

where

$$H = \mathbb{H}_0(\mathbf{div}; \Omega) := \left\{ \boldsymbol{\tau} \in \mathbb{H}(\mathbf{div}; \Omega) : \int_{\Omega} \text{tr}(\boldsymbol{\tau}) = 0 \right\},$$

$$X = \mathbb{L}_{\text{tr}}^2(\Omega) := \left\{ \mathbf{s} \in \mathbb{L}^2(\Omega) : \text{tr}(\mathbf{s}) = 0 \right\}, \quad \text{and} \quad Y := \mathbb{L}^2(\Omega).$$

In turn, $\mathcal{A} : (X \times H) \rightarrow (X \times H)' \equiv X' \times H'$ is the nonlinear operator

$$[\mathcal{A}(\mathbf{r}, \boldsymbol{\zeta}), (\mathbf{s}, \boldsymbol{\tau})] := 2 \int_{\Omega} \mu(|\mathbf{r}|) \mathbf{r} : \mathbf{s} - \int_{\Omega} \mathbf{s} : \boldsymbol{\zeta}^{\text{d}} + \int_{\Omega} \mathbf{r} : \boldsymbol{\tau}^{\text{d}} + \kappa \int_{\Omega} (\boldsymbol{\zeta}^{\text{d}} - 2\mu(|\mathbf{r}|) \mathbf{r}) : \boldsymbol{\tau}^{\text{d}}, \quad (2.7)$$

$\mathcal{B} : (X \times H) \rightarrow Y'$ is the linear operator

$$[\mathcal{B}(\mathbf{s}, \boldsymbol{\tau}), \mathbf{v}] := \int_{\Omega} \mathbf{v} \cdot \mathbf{div}(\boldsymbol{\tau}), \quad (2.8)$$

and the functionals $\mathcal{F} \in (X \times H)'$ and $\mathcal{G} \in Y'$ are given by

$$[\mathcal{F}, (\mathbf{s}, \boldsymbol{\tau})] := \langle \boldsymbol{\tau} \mathbf{n}, \mathbf{g} \rangle_{\Gamma} \quad \text{and} \quad [\mathcal{G}, \mathbf{v}] := - \int_{\Omega} \mathbf{f} \cdot \mathbf{v}, \quad (2.9)$$

for all $(\mathbf{r}, \boldsymbol{\zeta}), (\mathbf{s}, \boldsymbol{\tau}) \in X \times H$ and for all $\mathbf{v} \in Y$, where $[\cdot, \cdot]$ stands in each case for the duality pairing induced by the corresponding operators and functionals.

We remark here that the last expression appearing in the definition of \mathcal{A} (cf. (2.7)) rises precisely from the aforementioned further testing of the nonlinear constitutive law relating $\boldsymbol{\sigma}$ and \mathbf{t} (cf. first equation of (2.4)), which reduces to

$$\kappa \int_{\Omega} (\boldsymbol{\sigma}^{\text{d}} - 2\mu(|\mathbf{t}|) \mathbf{t}) : \boldsymbol{\tau}^{\text{d}} = 0 \quad \forall \boldsymbol{\tau} \in H. \quad (2.10)$$

Similarly as in [23], we highlight that the utilization of (2.10) in the derivation of (2.6) has yielded the aforementioned saddle-point type structure of our problem. Otherwise, the resulting variational formulation would be given by a twofold saddle point-type nonlinear system, in which case a second discrete inf-sup condition would need to be satisfied, thus additionally restricting the choice of the virtual element subspaces to be employed below. In other words, incorporating (2.10) into the variational formulation guarantees more freedom for defining our mixed virtual element scheme.

In addition, we now observe that we can write

$$[\mathcal{A}(\mathbf{r}, \boldsymbol{\zeta}), (\mathbf{s}, \boldsymbol{\tau})] := [\mathbf{A}(\mathbf{r}), \mathbf{s} - \kappa \boldsymbol{\tau}^{\text{d}}] - \int_{\Omega} \mathbf{s} : \boldsymbol{\zeta}^{\text{d}} + \int_{\Omega} \mathbf{r} : \boldsymbol{\tau}^{\text{d}} + \kappa \int_{\Omega} \boldsymbol{\zeta}^{\text{d}} : \boldsymbol{\tau}^{\text{d}} \quad (2.11)$$

for each $(\mathbf{r}, \boldsymbol{\zeta}), (\mathbf{s}, \boldsymbol{\tau}) \in X \times H$, where $\mathbf{A} : X \rightarrow X'$ is the auxiliary nonlinear operator defined by

$$[\mathbf{A}(\mathbf{r}), \mathbf{s}] := 2 \int_{\Omega} \mu(|\mathbf{r}|) \mathbf{r} : \mathbf{s} \quad \forall \mathbf{r}, \mathbf{s} \in X. \quad (2.12)$$

Furthermore, we know from [23, Lemma 2.1] that the operator \mathbf{A} is Lipschitz-continuous and strongly monotone. More precisely, with the constants γ_0 and α_0 specified in (2.2) and (2.3), respectively, there hold

$$\|\mathbf{A}(\mathbf{r}) - \mathbf{A}(\mathbf{s})\|_{X'} \leq 2\gamma_0 \|\mathbf{r} - \mathbf{s}\|_{0,\Omega} \quad (2.13)$$

and

$$[\mathbf{A}(\mathbf{r}) - \mathbf{A}(\mathbf{s}), \mathbf{r} - \mathbf{s}] \geq 2\alpha_0 \|\mathbf{r} - \mathbf{s}\|_{0,\Omega}^2, \quad (2.14)$$

for each $\mathbf{r}, \mathbf{s} \in X$.

The well-posedness of the augmented formulation (2.6) is established as follows.

Theorem 2.1. *Assume that the parameter κ defining the operator \mathcal{A} (cf. (2.11)) lies in $\left(0, \frac{\alpha_0}{\gamma_0}\right)$, where γ_0 and α_0 are the positive constants from (2.2) and (2.3). Then, there exists a unique $((\mathbf{t}, \boldsymbol{\sigma}), \mathbf{u}) \in (X \times H) \times Y$ solution of (2.6). Moreover, there exists $C > 0$ such that*

$$\|\mathbf{t}\|_{0,\Omega} + \|\boldsymbol{\sigma}\|_{\text{div};\Omega} + \|\mathbf{u}\|_{0,\Omega} \leq C \left\{ \|\mathbf{f}\|_{0,\Omega} + \|\mathbf{g}\|_{1/2,\Gamma} \right\}.$$

Proof. See [23, Theorem 3.2] □

3 The mixed virtual element method: an abstract approach

In this section we introduce and analyze an abstract mixed virtual element method for our continuous formulation (2.6). The *abstract* concept employed here refers to the fact that we consider generic virtual element subspaces and projectors satisfying certain conditions under which we prove the unique solvability of the discrete scheme and derive the associated *a priori* error estimates.

3.1 Preliminaries

Let $\{\mathcal{T}_h\}_{h>0}$ be a family of decompositions of Ω in polygonal elements. For each $K \in \mathcal{T}_h$ we denote its diameter by h_K , and define, as usual, $h := \max\{h_K : K \in \mathcal{T}_h\}$. In what follows we assume that there exists a constant $C_{\mathcal{T}} > 0$ such that for each decomposition \mathcal{T}_h and for each $K \in \mathcal{T}_h$ there hold:

- a) the ratio between the shortest edge and the diameter h_K of K is bigger than $C_{\mathcal{T}}$, and
- b) K is star-shaped with respect to a ball B of radius $C_{\mathcal{T}} h_K$ and center $\mathbf{x}_B \in K$, that is, for each $\mathbf{x}_0 \in B$, all the line segments joining \mathbf{x}_0 with any $\mathbf{x} \in K$ are contained in K , or, equivalently, for each $\mathbf{x} \in K$, the closed convex hull of $\{\mathbf{x}\} \cup B$ is contained in K .

As a consequence of the above hypotheses, one can show that each $K \in \mathcal{T}_h$ is simply connected, and that there exists an integer $N_{\mathcal{T}}$ (depending only on $C_{\mathcal{T}}$), such that the number of edges of each $K \in \mathcal{T}_h$ is bounded above by $N_{\mathcal{T}}$.

We now let $\prod_{K \in \mathcal{T}_h} X^K$, $\prod_{K \in \mathcal{T}_h} H^K$, and $\prod_{K \in \mathcal{T}_h} Y^K$ be finite dimensional subspaces of $\prod_{K \in \mathcal{T}_h} \mathbb{L}^2(K)$, $\prod_{K \in \mathcal{T}_h} \mathbb{H}(\text{div}; K)$, and $\prod_{K \in \mathcal{T}_h} \mathbb{L}^2(K)$, respectively, and define corresponding finite dimensional subspaces of X , H , and Y as

$$X_h := \left\{ \mathbf{s} \in X : \mathbf{s}|_K \in X^K \quad \forall K \in \mathcal{T}_h \right\}, \quad (3.1)$$

$$H_h := \left\{ \boldsymbol{\tau} \in H : \boldsymbol{\tau}|_K \in H^K \quad \forall K \in \mathcal{T}_h \right\}, \quad (3.2)$$

$$Y_h := \left\{ \mathbf{v} \in Y : \mathbf{v}|_K \in Y^K \quad \forall K \in \mathcal{T}_h \right\}. \quad (3.3)$$

In Section 4 below we present particular choices for X^K , H^K and Y^K . In this regard, we remark in advance that X^K and Y^K are going to be merely subspaces of certain spaces of polynomials, whereas that H^K will be given by a local virtual element space. Nevertheless, at this moment we simply assume that the following conditions hold:

(A.1) for each $K \in \mathcal{T}_h$ the elements of X^K and Y^K are explicitly known in the whole element K .

(A.2) for each $K \in \mathcal{T}_h$ and for each edge $e \in \partial K$, $\boldsymbol{\tau}\mathbf{n}|_e$ and $\mathbf{div}(\boldsymbol{\tau})$ are explicitly known for all $\boldsymbol{\tau} \in H^K$.

(A.3) $\mathbf{div}(H^K) \subseteq Y^K$ for each $K \in \mathcal{T}_h$.

(A.4) for each $K \in \mathcal{T}_h$ there exists a set of unisolvent degrees of freedom $\{m_{i,K}(\mathbf{v})\}_{i=1}^{n^K}$ of H^K , so that letting $\mathcal{S}^K : H^K \times H^K \rightarrow \mathbb{R}$ be the bilinear form associated to those degrees of freedom, that is

$$\mathcal{S}^K(\boldsymbol{\zeta}, \boldsymbol{\tau}) := \sum_{i=1}^{n^K} m_{i,K}(\boldsymbol{\zeta}) m_{i,K}(\boldsymbol{\tau}) \quad \forall \boldsymbol{\zeta}, \boldsymbol{\tau} \in H^K, \quad (3.4)$$

there holds

$$c_0 \|\boldsymbol{\zeta}\|_{0,K}^2 \leq \mathcal{S}^K(\boldsymbol{\zeta}, \boldsymbol{\zeta}) \leq c_1 \|\boldsymbol{\zeta}\|_{0,K}^2 \quad \forall \boldsymbol{\zeta} \in H^K, \quad (3.5)$$

with constants $c_0, c_1 > 0$, depending only on $C_{\mathcal{T}}$.

(A.5) for each $K \in \mathcal{T}_h$ there exists a subspace $\tilde{\mathbb{H}}(K)$ of $\mathbb{H}(\mathbf{div}; K)$ and a linear operator $\Pi^K : \tilde{\mathbb{H}}(K) \rightarrow H^K$ such that

$$\int_K \mathbf{v} \cdot \mathbf{div}(\Pi^K(\boldsymbol{\tau})) = \int_K \mathbf{v} \cdot \mathbf{div}(\boldsymbol{\tau}) \quad \forall \boldsymbol{\tau} \in \tilde{\mathbb{H}}(K), \quad \forall \mathbf{v} \in Y^K. \quad (3.6)$$

(A.6) there exists a subspace $\tilde{\mathbb{H}}(\Omega)$ of $\mathbb{H}(\mathbf{div}; \Omega)$ satisfying $\boldsymbol{\zeta}|_K \in \tilde{\mathbb{H}}(K) \quad \forall K \in \mathcal{T}_h, \quad \forall \boldsymbol{\zeta} \in \tilde{\mathbb{H}}(\Omega)$, and such that for each $h > 0$ the global counterpart Π^h of the family $\{\Pi^K\}_{K \in \mathcal{T}_h}$, that is the linear operator defined by

$$\Pi^h(\boldsymbol{\zeta})|_K := \Pi^K(\boldsymbol{\zeta}|_K) \quad \forall K \in \mathcal{T}_h, \quad \forall \boldsymbol{\zeta} \in \tilde{\mathbb{H}}(\Omega),$$

maps $\tilde{\mathbb{H}}(\Omega)$ into H_h .

3.2 The discrete scheme

We now aim to define a Galerkin scheme for our nonlinear problem (2.6). To this end, we first notice thanks to (A.1) and (A.2) that the linear operator \mathcal{B} (cf. (2.8)) and the functionals \mathcal{F} and \mathcal{G} (cf. (2.9)) are all explicitly computable for $(\mathbf{s}, \boldsymbol{\tau}, \mathbf{v}) \in X_h \times H_h \times Y_h$ (cf. (3.1), (3.2), and (3.3)). On the contrary, for each $K \in \mathcal{T}_h$, the local version $\mathcal{A}^K : (X^K \times H^K) \rightarrow (X^K \times H^K)'$ of the nonlinear operator \mathcal{A} (cf. (2.11)), which is defined for each $(\mathbf{r}, \boldsymbol{\zeta}), (\mathbf{s}, \boldsymbol{\tau}) \in X^K \times H^K$ by

$$[\mathcal{A}^K(\mathbf{r}, \boldsymbol{\zeta}), (\mathbf{s}, \boldsymbol{\tau})] := 2 \int_K \mu(|\mathbf{r}|) \mathbf{r} : (\mathbf{s} - \kappa \boldsymbol{\tau}^d) - \int_K \boldsymbol{\zeta}^d : \mathbf{s} + \int_K \boldsymbol{\tau}^d : \mathbf{r} + \kappa \int_K \boldsymbol{\zeta}^d : \boldsymbol{\tau}^d, \quad (3.7)$$

is not explicitly calculable for $\boldsymbol{\zeta}, \boldsymbol{\tau} \in H^K$ since in general $\boldsymbol{\zeta}$ and $\boldsymbol{\tau}$ are not necessarily known on the whole $K \in \mathcal{T}_h$. In order to deal with this difficulty, we now consider a suitable space \hat{H}^K on which the elements of H^K will be projected later on, and such that the operator \mathcal{A}^K is computable in $X^K \times \hat{H}^K$. More precisely, for each $K \in \mathcal{T}_h$ we let \hat{H}^K be a finite dimensional subspace of $\mathbb{H}(\mathbf{div}; K)$, and assume that there exists a projection operator $\hat{\Pi}^K : \mathbb{H}(\mathbf{div}; K) \rightarrow \hat{H}^K$ satisfying the following properties:

(P.1) for each $\boldsymbol{\zeta} \in H^K$, $\hat{\Pi}^K(\boldsymbol{\zeta})$ is explicitly calculable.

(P.2) for each $\boldsymbol{\zeta} \in \mathbb{H}(\mathbf{div}; K)$ there holds

$$\|\hat{\Pi}^K(\boldsymbol{\zeta})\|_{0,K} \leq \hat{c}_1 \|\boldsymbol{\zeta}\|_{0,K} + \hat{c}_2 h_K \|\mathbf{div}(\boldsymbol{\zeta})\|_{0,K} \quad (3.8)$$

with constants $\hat{c}_1 > 0$ and $\hat{c}_2 \geq 0$, independent of K .

(P.3) for each $\zeta \in \mathbb{H}(\mathbf{div}; K)$ there holds

$$\int_K (\zeta - \widehat{\Pi}^K(\zeta)) : \mathbf{s} = 0 \quad \forall \mathbf{s} \in X^K. \quad (3.9)$$

It is worth mentioning at this point that the assumptions **(P.2)** and **(P.3)** will be utilized to establish the solvability analysis and derive the corresponding *a priori* error estimates of the discrete scheme to be defined below in (3.12). In turn, two particular choices for the spaces \widehat{H}^K and associated projections $\widehat{\Pi}^K$ are provided in Section 4 (though only one of them will work for the present nonlinear model).

Next, having introduced \widehat{H}^K and $\widehat{\Pi}^K$ for each $K \in \mathcal{T}_h$, we now let $\mathcal{A}_h^K : (X^K \times H^K) \rightarrow (X^K \times H^K)'$ be the computable local discrete nonlinear operator approximating (3.7), which, following [12, eq. (4.18)], is defined by

$$[\mathcal{A}_h^K(\mathbf{r}, \zeta), (\mathbf{s}, \boldsymbol{\tau})] := [\mathcal{A}^K(\mathbf{r}, \widehat{\Pi}^K(\zeta)), (\mathbf{s}, \widehat{\Pi}^K(\boldsymbol{\tau}))] + \kappa \mathcal{S}^K(\zeta - \widehat{\Pi}^K(\zeta), \boldsymbol{\tau} - \widehat{\Pi}^K(\boldsymbol{\tau})) \quad (3.10)$$

for all $(\mathbf{r}, \zeta), (\mathbf{s}, \boldsymbol{\tau}) \in X^K \times H^K$, where $\mathcal{S}^K : H^K \times H^K \rightarrow \mathbb{R}$ is the stabilizing bilinear form given in (3.4), and $\kappa > 0$ is the parameter utilized in the augmented equation (2.10). The reason why κ has been placed here, multiplying \mathcal{S}^K , is just for sake of convenience in a particular algebraic manipulation to be explained later on (see below (3.21) and the remark after it). According to the definition (3.10), we now introduce the global discrete nonlinear operator $\mathcal{A}_h : (X_h \times H_h) \rightarrow (X_h \times H_h)'$ as

$$[\mathcal{A}_h(\mathbf{r}, \zeta), (\mathbf{s}, \boldsymbol{\tau})] := \sum_{K \in \mathcal{T}_h} [\mathcal{A}_h^K(\mathbf{r}, \zeta), (\mathbf{s}, \boldsymbol{\tau})] \quad \forall (\mathbf{r}, \zeta), (\mathbf{s}, \boldsymbol{\tau}) \in X_h \times H_h. \quad (3.11)$$

In this way, the Galerkin scheme associated with the augmented formulation (2.6) reads: Find $((\mathbf{t}_h, \boldsymbol{\sigma}_h), \mathbf{u}_h) \in (X_h \times H_h) \times Y_h$ such that

$$\begin{aligned} [\mathcal{A}_h(\mathbf{t}_h, \boldsymbol{\sigma}_h), (\mathbf{s}_h, \boldsymbol{\tau}_h)] + [\mathcal{B}(\mathbf{s}_h, \boldsymbol{\tau}_h), \mathbf{u}_h] &= [\mathcal{F}, (\mathbf{s}_h, \boldsymbol{\tau}_h)] & \forall (\mathbf{s}_h, \boldsymbol{\tau}_h) \in X_h \times H_h, \\ [\mathcal{B}(\mathbf{t}_h, \boldsymbol{\sigma}_h), \mathbf{v}_h] &= [\mathcal{G}, \mathbf{v}_h] & \forall \mathbf{v}_h \in Y_h. \end{aligned} \quad (3.12)$$

Moreover, as suggested by (2.5), the postprocessed virtual pressure is given by

$$p_h := -\frac{1}{2} \text{tr}(\boldsymbol{\sigma}_h). \quad (3.13)$$

3.3 Analysis of the discrete scheme

In this section we develop the solvability analysis for our augmented Galerkin scheme (3.12). For this purpose, we first notice that the discrete kernel of \mathcal{B} (cf. (2.8)), defined by

$$V_h := \left\{ (\mathbf{s}_h, \boldsymbol{\tau}_h) \in X_h \times H_h : [\mathcal{B}(\mathbf{s}_h, \boldsymbol{\tau}_h), \mathbf{v}_h] = 0 \quad \forall \mathbf{v}_h \in Y_h \right\},$$

reduces to

$$V_h = X_h \times \left\{ \boldsymbol{\tau}_h \in H_h : \int_{\Omega} \mathbf{v}_h \cdot \mathbf{div}(\boldsymbol{\tau}_h) = 0 \quad \forall \mathbf{v}_h \in Y_h \right\},$$

which, thanks to **(A.3)**, becomes

$$V_h = X_h \times \left\{ \boldsymbol{\tau}_h \in H_h : \mathbf{div}(\boldsymbol{\tau}_h) = \mathbf{0} \right\}. \quad (3.14)$$

Furthermore, given the local projector $\widehat{\Pi}^K$ introduced in Section 3.2, we denote by $\widehat{\Pi}^h$ its global counterpart, that is, for each $\boldsymbol{\zeta} \in \mathbb{H}(\mathbf{div}; \Omega)$ we let

$$\widehat{\Pi}^h(\boldsymbol{\zeta})|_K := \widehat{\Pi}^K(\boldsymbol{\zeta}|_K) \quad \forall K \in \mathcal{T}_h.$$

The following result establishes the Lipschitz-continuity of the discrete nonlinear operator \mathcal{A}_h (cf. (3.11)) on $X_h \times H_h$.

Lemma 3.1. *Let \mathcal{A}_h be the nonlinear operator defined by (3.11). Then, there exists a constant $\gamma > 0$, independent of h , such that for all $(\mathbf{r}, \boldsymbol{\zeta}), (\mathbf{s}, \boldsymbol{\tau}) \in X_h \times H_h$ there holds*

$$\|\mathcal{A}_h(\mathbf{r}, \boldsymbol{\zeta}) - \mathcal{A}_h(\mathbf{s}, \boldsymbol{\tau})\|_{(X \times H)'} \leq \gamma \|(\mathbf{r}, \boldsymbol{\zeta}) - (\mathbf{s}, \boldsymbol{\tau})\|_{X \times H}. \quad (3.15)$$

Proof. Given $(\mathbf{r}, \boldsymbol{\zeta}), (\mathbf{s}, \boldsymbol{\tau}) \in X_h \times H_h$, we first recall that

$$\|\mathcal{A}_h(\mathbf{r}, \boldsymbol{\zeta}) - \mathcal{A}_h(\mathbf{s}, \boldsymbol{\tau})\|_{(X \times H)'} := \sup_{\substack{(\mathbf{z}, \boldsymbol{\rho}) \in X \times H \\ (\mathbf{z}, \boldsymbol{\rho}) \neq \mathbf{0}}} \frac{[\mathcal{A}_h(\mathbf{r}, \boldsymbol{\zeta}) - \mathcal{A}_h(\mathbf{s}, \boldsymbol{\tau}), (\mathbf{z}, \boldsymbol{\rho})]}{\|(\mathbf{z}, \boldsymbol{\rho})\|_{X \times H}}. \quad (3.16)$$

In turn, according to the definitions of \mathcal{A}_h (cf. (3.11)) and \mathbf{A} (cf. (2.12)), we have that

$$\begin{aligned} [\mathcal{A}_h(\mathbf{r}, \boldsymbol{\zeta}) - \mathcal{A}_h(\mathbf{s}, \boldsymbol{\tau}), (\mathbf{z}, \boldsymbol{\rho})] &= [\mathbf{A}(\mathbf{r}) - \mathbf{A}(\mathbf{s}), \mathbf{z} - \kappa(\widehat{\Pi}^h(\boldsymbol{\rho}))^{\mathbf{d}}] - \int_{\Omega} (\widehat{\Pi}^h(\boldsymbol{\zeta} - \boldsymbol{\tau}))^{\mathbf{d}} : \mathbf{z} \\ &+ \int_{\Omega} (\widehat{\Pi}^h(\boldsymbol{\rho}))^{\mathbf{d}} : (\mathbf{r} - \mathbf{s}) + \kappa \int_{\Omega} (\widehat{\Pi}^h(\boldsymbol{\zeta} - \boldsymbol{\tau}))^{\mathbf{d}} : (\widehat{\Pi}^h(\boldsymbol{\rho}))^{\mathbf{d}} \\ &+ \kappa \sum_{K \in \mathcal{T}_h} \mathcal{S}^K((\mathbf{I} - \widehat{\Pi}^K)(\boldsymbol{\zeta} - \boldsymbol{\tau}), (\mathbf{I} - \widehat{\Pi}^K)(\boldsymbol{\rho})) \end{aligned} \quad (3.17)$$

for all $(\mathbf{z}, \boldsymbol{\rho}) \in X \times H$. Next, employing the Cauchy-Schwarz inequality, in particular the estimate

$$\mathcal{S}^K(\boldsymbol{\zeta}, \boldsymbol{\tau}) \leq \mathcal{S}^K(\boldsymbol{\zeta}, \boldsymbol{\zeta})^{1/2} \mathcal{S}^K(\boldsymbol{\tau}, \boldsymbol{\tau})^{1/2} \quad \forall \boldsymbol{\zeta}, \boldsymbol{\tau} \in \mathbb{H}(\mathbf{div}; K) \quad \forall K \in \mathcal{T}_h,$$

which is actually valid not only for \mathcal{S}^K , but for any positive semi-definite bilinear form, and using the Lipschitz-continuity of \mathbf{A} (cf. (2.13)), and the fact that $\|\boldsymbol{\tau}^{\mathbf{d}}\|_{0, \Omega} \leq \|\boldsymbol{\tau}\|_{0, \Omega} \quad \forall \boldsymbol{\tau} \in \mathbb{H}(\mathbf{div}; \Omega)$, we readily find that

$$\begin{aligned} [\mathcal{A}_h(\mathbf{r}, \boldsymbol{\zeta}) - \mathcal{A}_h(\mathbf{s}, \boldsymbol{\tau}), (\mathbf{z}, \boldsymbol{\rho})] &\leq 2\gamma_0 \|\mathbf{r} - \mathbf{s}\|_{0, \Omega} \|\mathbf{z}\|_{0, \Omega} + 2\gamma_0 \kappa \|\mathbf{r} - \mathbf{s}\|_{0, \Omega} \|\widehat{\Pi}^h(\boldsymbol{\rho})\|_{0, \Omega} \\ &+ \|\widehat{\Pi}^h(\boldsymbol{\zeta} - \boldsymbol{\tau})\|_{0, \Omega} \|\mathbf{z}\|_{0, \Omega} + \|\mathbf{r} - \mathbf{s}\|_{0, \Omega} \|\widehat{\Pi}^h(\boldsymbol{\rho})\|_{0, \Omega} + \kappa \|\widehat{\Pi}^h(\boldsymbol{\zeta} - \boldsymbol{\tau})\|_{0, \Omega} \|\widehat{\Pi}^h(\boldsymbol{\rho})\|_{0, \Omega} \\ &+ \kappa \sum_{K \in \mathcal{T}_h} \left\{ \mathcal{S}^K((\mathbf{I} - \widehat{\Pi}^K)(\boldsymbol{\zeta} - \boldsymbol{\tau}), (\mathbf{I} - \widehat{\Pi}^K)(\boldsymbol{\zeta} - \boldsymbol{\tau})) \right\}^{1/2} \left\{ \mathcal{S}^K((\mathbf{I} - \widehat{\Pi}^K)(\boldsymbol{\rho}), (\mathbf{I} - \widehat{\Pi}^K)(\boldsymbol{\rho})) \right\}^{1/2}. \end{aligned}$$

Then, applying the upper bound of (3.5) and reordering terms, we deduce that

$$\begin{aligned} [\mathcal{A}_h(\mathbf{r}, \boldsymbol{\zeta}) - \mathcal{A}_h(\mathbf{s}, \boldsymbol{\tau}), (\mathbf{z}, \boldsymbol{\rho})] &\leq C \left\{ \|\mathbf{r} - \mathbf{s}\|_{0, \Omega} + \|\widehat{\Pi}^h(\boldsymbol{\zeta} - \boldsymbol{\tau})\|_{0, \Omega} \right. \\ &\left. + \|(\mathbf{I} - \widehat{\Pi}^h)(\boldsymbol{\zeta} - \boldsymbol{\tau})\|_{0, \Omega} \right\} \left\{ \|\mathbf{z}\|_{0, \Omega} + \|\widehat{\Pi}^h(\boldsymbol{\rho})\|_{0, \Omega} + \|(\mathbf{I} - \widehat{\Pi}^h)(\boldsymbol{\rho})\|_{0, \Omega} \right\}, \end{aligned} \quad (3.18)$$

from which, using the boundedness of $\widehat{\Pi}^h$ (cf. (3.8) in **(P.2)**), we arrive at

$$[\mathcal{A}_h(\mathbf{r}, \boldsymbol{\zeta}) - \mathcal{A}_h(\mathbf{s}, \boldsymbol{\tau}), (\mathbf{z}, \boldsymbol{\rho})] \leq \gamma \|(\mathbf{r}, \boldsymbol{\zeta}) - (\mathbf{s}, \boldsymbol{\tau})\|_{X \times H} \|(\mathbf{z}, \boldsymbol{\rho})\|_{X \times H} \quad \forall (\mathbf{z}, \boldsymbol{\rho}) \in X \times H, \quad (3.19)$$

with a constant γ depending on $\gamma_0, \kappa, c_1, \widehat{c}_1$, and \widehat{c}_2 . Finally, it is clear that the required inequality (3.15) follows straightforwardly from (3.16) and (3.19). \square

At this point we remark in advance that the intermediate inequality (3.18) will play later on an important role in the derivation of the *a priori* error estimates (see Section 3.4). We now proceed with our analysis by recalling the following technical result.

Lemma 3.2. *There exists $c_\Omega > 0$, depending only on Ω , such that*

$$c_\Omega \|\boldsymbol{\tau}\|_{0,\Omega}^2 \leq \|\boldsymbol{\tau}^d\|_{0,\Omega}^2 + \|\mathbf{div}(\boldsymbol{\tau})\|_{0,\Omega}^2 \quad \forall \boldsymbol{\tau} \in H.$$

Proof. See [10, Chapter IV, Proposition 3.1]. □

The following lemma establishes a sufficient condition on the parameter κ ensuring that for each $(\mathbf{r}_0, \boldsymbol{\zeta}_0) \in X_h \times H_h$, the nonlinear operator $\mathcal{A}_h((\mathbf{r}_0, \boldsymbol{\zeta}_0) + \cdot)$ is uniformly strongly monotone on the discrete kernel V_h of \mathcal{B} .

Lemma 3.3. *Let \mathcal{A}_h and \mathcal{B} be the operators defined by (3.11) and (2.8), respectively, and let V_h be the discrete kernel of \mathcal{B} (cf. (3.14)). Assume that the parameter κ lies in $(0, \frac{\alpha_0}{\gamma_0})$, where γ_0 and α_0 are the positive constants from (2.2) and (2.3). Then, there exists a constant $\alpha > 0$, independent of h , such that*

$$[\mathcal{A}_h((\mathbf{r}_0, \boldsymbol{\zeta}_0) + (\mathbf{r}, \boldsymbol{\zeta})) - \mathcal{A}_h((\mathbf{r}_0, \boldsymbol{\zeta}_0) + (\mathbf{s}, \boldsymbol{\tau}))], (\mathbf{r}, \boldsymbol{\zeta}) - (\mathbf{s}, \boldsymbol{\tau})] \geq \alpha \|(\mathbf{r}, \boldsymbol{\zeta}) - (\mathbf{s}, \boldsymbol{\tau})\|_{X \times H}^2$$

for each $(\mathbf{r}_0, \boldsymbol{\zeta}_0) \in X_h \times H_h$ and for all $(\mathbf{r}, \boldsymbol{\zeta}), (\mathbf{s}, \boldsymbol{\tau}) \in V_h$.

Proof. Given $(\mathbf{r}_0, \boldsymbol{\zeta}_0) \in X_h \times H_h$ and $(\mathbf{r}, \boldsymbol{\zeta}), (\mathbf{s}, \boldsymbol{\tau}) \in V_h$, it follows from the definitions of \mathcal{A}_h (cf. (3.11)) and \mathbf{A} (cf. (2.12)) (see also (3.17)) that

$$\begin{aligned} & [\mathcal{A}_h((\mathbf{r}_0, \boldsymbol{\zeta}_0) + (\mathbf{r}, \boldsymbol{\zeta})) - \mathcal{A}_h((\mathbf{r}_0, \boldsymbol{\zeta}_0) + (\mathbf{s}, \boldsymbol{\tau}))], (\mathbf{r}, \boldsymbol{\zeta}) - (\mathbf{s}, \boldsymbol{\tau})] \\ &= [\mathbf{A}(\mathbf{r}_0 + \mathbf{r}) - \mathbf{A}(\mathbf{r}_0 + \mathbf{s}), \mathbf{r} - \mathbf{s}] - \kappa [\mathbf{A}(\mathbf{r}_0 + \mathbf{r}) - \mathbf{A}(\mathbf{r}_0 + \mathbf{s}), (\widehat{\Pi}^h(\boldsymbol{\zeta} - \boldsymbol{\tau}))^d] \\ &+ \kappa \|(\widehat{\Pi}^h(\boldsymbol{\zeta} - \boldsymbol{\tau}))^d\|_{0,\Omega}^2 + \kappa \sum_{K \in \mathcal{T}_h} \mathcal{S}^K((I - \widehat{\Pi}^K)(\boldsymbol{\zeta} - \boldsymbol{\tau}), (I - \widehat{\Pi}^K)(\boldsymbol{\zeta} - \boldsymbol{\tau})). \end{aligned} \quad (3.20)$$

Then, using that

$$[\mathbf{A}(\mathbf{r}_0 + \mathbf{r}) - \mathbf{A}(\mathbf{r}_0 + \mathbf{s}), \mathbf{r} - \mathbf{s}] = [\mathbf{A}(\mathbf{r}_0 + \mathbf{r}) - \mathbf{A}(\mathbf{r}_0 + \mathbf{s}), (\mathbf{r}_0 + \mathbf{r}) - (\mathbf{r}_0 + \mathbf{s})],$$

and applying the Lipschitz-continuity (cf. (2.13)) and strong monotonicity (cf. (2.14)) of \mathbf{A} , we deduce from (3.20) that

$$\begin{aligned} & [\mathcal{A}_h((\mathbf{r}_0, \boldsymbol{\zeta}_0) + (\mathbf{r}, \boldsymbol{\zeta})) - \mathcal{A}_h((\mathbf{r}_0, \boldsymbol{\zeta}_0) + (\mathbf{s}, \boldsymbol{\tau}))], (\mathbf{r}, \boldsymbol{\zeta}) - (\mathbf{s}, \boldsymbol{\tau})] \\ & \geq 2\alpha_0 \|\mathbf{r} - \mathbf{s}\|_{0,\Omega}^2 - 2\gamma_0 \kappa \|\mathbf{r} - \mathbf{s}\|_{0,\Omega} \|(\widehat{\Pi}^h(\boldsymbol{\zeta} - \boldsymbol{\tau}))^d\|_{0,\Omega} \\ & + \kappa \|(\widehat{\Pi}^h(\boldsymbol{\zeta} - \boldsymbol{\tau}))^d\|_{0,\Omega}^2 + \kappa \sum_{K \in \mathcal{T}_h} \mathcal{S}^K((I - \widehat{\Pi}^K)(\boldsymbol{\zeta} - \boldsymbol{\tau}), (I - \widehat{\Pi}^K)(\boldsymbol{\zeta} - \boldsymbol{\tau})) \\ & \geq 2\alpha_0 \|\mathbf{r} - \mathbf{s}\|_{0,\Omega}^2 - 2\gamma_0 \kappa \left\{ \frac{\|\mathbf{r} - \mathbf{s}\|_{0,\Omega}^2}{2\delta} + \frac{\delta \|(\widehat{\Pi}^h(\boldsymbol{\zeta} - \boldsymbol{\tau}))^d\|_{0,\Omega}^2}{2} \right\} \\ & + \kappa \|(\widehat{\Pi}^h(\boldsymbol{\zeta} - \boldsymbol{\tau}))^d\|_{0,\Omega}^2 + \kappa \sum_{K \in \mathcal{T}_h} \mathcal{S}^K((I - \widehat{\Pi}^K)(\boldsymbol{\zeta} - \boldsymbol{\tau}), (I - \widehat{\Pi}^K)(\boldsymbol{\zeta} - \boldsymbol{\tau})) \\ & = \left(2\alpha_0 - \frac{\gamma_0 \kappa}{\delta} \right) \|\mathbf{r} - \mathbf{s}\|_{0,\Omega}^2 + \kappa(1 - \gamma_0 \delta) \|(\widehat{\Pi}^h(\boldsymbol{\zeta} - \boldsymbol{\tau}))^d\|_{0,\Omega}^2 \\ & + \kappa \sum_{K \in \mathcal{T}_h} \mathcal{S}^K((I - \widehat{\Pi}^K)(\boldsymbol{\zeta} - \boldsymbol{\tau}), (I - \widehat{\Pi}^K)(\boldsymbol{\zeta} - \boldsymbol{\tau})), \end{aligned}$$

where $\delta > 0$ is a constant to be suitable chosen. Indeed, we realize now that in order to obtain positive constants multiplying the first two expressions after the last equal sign, it suffices to choose $\delta \in \left(0, \frac{1}{\gamma_0}\right)$ and $\kappa \in \left(0, \frac{2\alpha_0\delta}{\gamma_0}\right)$. In particular, for $\delta = \frac{1}{2\gamma_0}$ we require $\kappa \in \left(0, \frac{\alpha_0}{\gamma_0^2}\right)$, whence we find that

$$\begin{aligned}
& [\mathcal{A}_h((\mathbf{r}_0, \zeta_0) + (\mathbf{r}, \zeta)) - \mathcal{A}_h((\mathbf{r}_0, \zeta_0) + (\mathbf{s}, \tau)), (\mathbf{r}, \zeta) - (\mathbf{s}, \tau)] \\
& \geq 2(\alpha_0 - \kappa\gamma_0^2) \|\mathbf{r} - \mathbf{s}\|_{0,\Omega}^2 + \frac{\kappa}{2} \|(\widehat{\Pi}^h(\zeta - \tau))^d\|_{0,\Omega}^2 \\
& + \kappa \sum_{K \in \mathcal{T}_h} \mathcal{S}^K((\mathbf{I} - \widehat{\Pi}^K)(\zeta - \tau), (\mathbf{I} - \widehat{\Pi}^K)(\zeta - \tau)) \\
& \geq 2(\alpha_0 - \kappa\gamma_0^2) \|\mathbf{r} - \mathbf{s}\|_{0,\Omega}^2 + \frac{\kappa}{2} \sum_{K \in \mathcal{T}_h} \left\{ \|(\widehat{\Pi}^K(\zeta - \tau))^d\|_{0,K}^2 \right. \\
& \left. + \mathcal{S}^K((\mathbf{I} - \widehat{\Pi}^K)(\zeta - \tau), (\mathbf{I} - \widehat{\Pi}^K)(\zeta - \tau)) \right\}.
\end{aligned} \tag{3.21}$$

Note that the previous incorporation of κ in the definition (3.10) is only to be able to factorize here by a multiple of this parameter. Actually, alternatively to bounding below by $\frac{\kappa}{2}$ in (3.21), it would have sufficed to use $\frac{\kappa}{2}$ instead of κ in (3.10). We employed the latter just for simplicity. On the other hand, a simple triangle inequality and the lower estimate in (3.5) imply that

$$\begin{aligned}
\|(\zeta - \tau)^d\|_{0,K}^2 & \leq 2 \left\{ \|(\widehat{\Pi}^K(\zeta - \tau))^d\|_{0,K}^2 + \|(\mathbf{I} - \widehat{\Pi}^K)(\zeta - \tau)\|_{0,K}^2 \right\} \\
& \leq 2 \left\{ \|(\widehat{\Pi}^K(\zeta - \tau))^d\|_{0,K}^2 + \|(\mathbf{I} - \widehat{\Pi}^K)(\zeta - \tau)\|_{0,K}^2 \right\} \\
& \leq 2 \max\{1, c_0^{-1}\} \left\{ \|(\widehat{\Pi}^K(\zeta - \tau))^d\|_{0,K}^2 + \mathcal{S}^K((\mathbf{I} - \widehat{\Pi}^K)(\zeta - \tau), (\mathbf{I} - \widehat{\Pi}^K)(\zeta - \tau)) \right\},
\end{aligned}$$

from which, summing over all $K \in \mathcal{T}_h$ and then applying Lemma 3.2 (bearing in mind that $\zeta - \tau$ is divergence free), we deduce that

$$\begin{aligned}
& \frac{c_\Omega}{2 \max\{1, c_0^{-1}\}} \|\zeta - \tau\|_{\text{div};\Omega}^2 \\
& \leq \sum_{K \in \mathcal{T}_h} \left\{ \|(\widehat{\Pi}^K(\zeta - \tau))^d\|_{0,K}^2 + \mathcal{S}^K((\mathbf{I} - \widehat{\Pi}^K)(\zeta - \tau), (\mathbf{I} - \widehat{\Pi}^K)(\zeta - \tau)) \right\}.
\end{aligned}$$

In this way, (3.21) and the foregoing inequality complete the proof of the required estimate with the strong monotonicity constant $\alpha := \min\left\{2(\alpha_0 - \kappa\gamma_0^2), \frac{\kappa c_\Omega}{4 \max\{1, c_0^{-1}\}}\right\}$. \square

The following lemma provides the discrete inf-sup condition for the linear operator \mathcal{B} (cf. (2.8)).

Lemma 3.4. *There exists $\beta > 0$, independent of h , such that*

$$\sup_{\substack{(\mathbf{s}_h, \boldsymbol{\tau}_h) \in X_h \times H_h \\ (\mathbf{s}_h, \boldsymbol{\tau}_h) \neq \mathbf{0}}} \frac{[\mathcal{B}(\mathbf{s}_h, \boldsymbol{\tau}_h), \mathbf{v}_h]}{\|(\mathbf{s}_h, \boldsymbol{\tau}_h)\|_{X \times H}} \geq \beta \|\mathbf{v}_h\|_{0,\Omega} \quad \forall \mathbf{v}_h \in Y_h.$$

Proof. We begin by recalling from (2.8) that \mathcal{B} does not depend on \mathbf{s}_h , and hence it suffices to show the existence of $\beta > 0$ such that

$$\sup_{\substack{\boldsymbol{\tau}_h \in H_h \\ \boldsymbol{\tau}_h \neq \mathbf{0}}} \frac{\int_{\Omega} \mathbf{v}_h \cdot \text{div}(\boldsymbol{\tau}_h)}{\|\boldsymbol{\tau}_h\|_{\text{div};\Omega}} \geq \beta \|\mathbf{v}_h\|_{0,\Omega} \quad \forall \mathbf{v}_h \in Y_h,$$

which, thanks to (A.5) and (A.6), follows as in the proof of [12, Lemma 5.3]. We omit further details. \square

The well-posedness of our Galerkin scheme (3.12) is established as follows.

Theorem 3.1. *Assume that the parameter κ defining the operator \mathcal{A}_h (cf. (3.11)) lies in $(0, \frac{\alpha_0}{\gamma_0^2})$, where γ_0 and α_0 are the positive constants from (2.2) and (2.3), respectively. Then, there exists a unique $((\mathbf{t}_h, \boldsymbol{\sigma}_h), \mathbf{u}_h) \in (X_h \times H_h) \times Y_h$ solution of (3.12). Moreover, there exists $C > 0$, depending on γ (cf. Lemma (3.1)), α (cf. Lemma (3.3)), and β (cf. Lemma (3.4)), such that*

$$\|\mathbf{t}_h\|_{0,\Omega} + \|\boldsymbol{\sigma}_h\|_{\text{div};\Omega} + \|\mathbf{u}_h\|_{0,\Omega} \leq C \left\{ \|\mathbf{f}\|_{0,\Omega} + \|\mathbf{g}\|_{1/2,\Gamma} \right\}.$$

Proof. Thanks to Lemmas 3.1, 3.3 and 3.4, the proof is a direct application of [23, Theorem 3.1] (which is a particular case of [30, Proposition 2.3]). \square

3.4 The a priori error estimates

We now aim to provide the corresponding *a priori* error estimates for the continuous and discrete formulations (2.6) and (3.12), respectively. To this end, in what follows we let $\mathcal{P}_X^h : X \rightarrow X_h$ and $\mathcal{P}_Y^h : Y \rightarrow Y_h$ be the orthogonal projectors with respect to the $\mathbb{L}^2(\Omega)$ and $\mathbb{L}^2(\Omega)$ inner products, respectively. In turn, we recall from (A.6) the definition of the global counterpart Π^h of the family of local operators $\{\Pi^K\}_{K \in \mathcal{T}_h}$ (cf. (A.5)), and notice, thanks to (A.3), (3.6), and (A.6) that there holds

$$\text{div}(\Pi^h(\boldsymbol{\zeta})) = \mathcal{P}_Y^h(\text{div}(\boldsymbol{\zeta})) \quad \text{in } \Omega, \quad \forall \boldsymbol{\zeta} \in \tilde{\mathbb{H}}(\Omega). \quad (3.22)$$

We begin our analysis with the following result.

Theorem 3.2. *Let $((\mathbf{t}, \boldsymbol{\sigma}), \mathbf{u}) \in (X \times H) \times Y$ and $((\mathbf{t}_h, \boldsymbol{\sigma}_h), \mathbf{u}_h) \in (X_h \times H_h) \times Y_h$ be the unique solutions of the continuous and discrete schemes (2.6) and (3.12), respectively, assume that $\boldsymbol{\sigma} \in \tilde{\mathbb{H}}(\Omega)$, and let $p_h \in L^2(\Omega)$ be the postprocessed virtual pressure defined in (3.13). Then, there exists $C > 0$, independent of h , such that*

$$\begin{aligned} & \|\mathbf{t} - \mathbf{t}_h\|_{0,\Omega} + \|\boldsymbol{\sigma} - \boldsymbol{\sigma}_h\|_{0,\Omega} + \|p - p_h\|_{0,\Omega} \\ & \leq C \left\{ \|\mathbf{t} - \mathcal{P}_X^h(\mathbf{t})\|_{0,\Omega} + \|\boldsymbol{\sigma} - \Pi^h(\boldsymbol{\sigma})\|_{0,\Omega} + \|\boldsymbol{\sigma} - \hat{\Pi}^h(\boldsymbol{\sigma})\|_{0,\Omega} + h \|\mathbf{f} - \mathcal{P}_Y^h(\mathbf{f})\|_{0,\Omega} \right\}, \end{aligned} \quad (3.23)$$

and there holds

$$\|\text{div}(\boldsymbol{\sigma} - \boldsymbol{\sigma}_h)\|_{0,\Omega} = \|\mathbf{f} - \mathcal{P}_Y^h(\mathbf{f})\|_{0,\Omega}. \quad (3.24)$$

Proof. We begin by observing, due to the triangle inequality, that

$$\|\mathbf{t} - \mathbf{t}_h\|_{0,\Omega} + \|\boldsymbol{\sigma} - \boldsymbol{\sigma}_h\|_{0,\Omega} \leq \|\mathbf{t} - \mathcal{P}_X^h(\mathbf{t})\|_{0,\Omega} + \|\boldsymbol{\sigma} - \Pi^h(\boldsymbol{\sigma})\|_{0,\Omega} + \|\boldsymbol{\delta}_h^{\mathbf{t}}\|_{0,\Omega} + \|\boldsymbol{\delta}_h^{\boldsymbol{\sigma}}\|_{0,\Omega}, \quad (3.25)$$

where $(\boldsymbol{\delta}_h^{\mathbf{t}}, \boldsymbol{\delta}_h^{\boldsymbol{\sigma}}) := (\mathcal{P}_X^h(\mathbf{t}) - \mathbf{t}_h, \Pi^h(\boldsymbol{\sigma}) - \boldsymbol{\sigma}_h) \in X_h \times H_h$. Next, employing (3.22), the second equations of (2.6) and (3.12), and the assumption (A.3), we deduce that

$$\text{div}(\Pi^h(\boldsymbol{\sigma})) = \mathcal{P}_Y^h(\text{div}(\boldsymbol{\sigma})) = \mathcal{P}_Y^h(-\mathbf{f}) = \text{div}(\boldsymbol{\sigma}_h),$$

which says that $(\boldsymbol{\delta}_h^{\mathbf{t}}, \boldsymbol{\delta}_h^{\boldsymbol{\sigma}}) \in V_h$ (cf. (3.14)). Note here that the identity (3.24) follows straightforwardly from the last equality and the fact that $\text{div}(\boldsymbol{\sigma}) = -\mathbf{f}$. Then, applying the strong monotonicity of \mathcal{A}_h (cf.

Lemma 3.3) with $(\mathbf{r}_0, \zeta_0) := (\mathbf{0}, \mathbf{0}) \in X_h \times H_h$, $(\mathbf{r}, \zeta) := (\mathcal{P}_X^h(\mathbf{t}), \delta_h^\sigma) \in V_h$, and $(\mathbf{s}, \tau) := (\mathbf{t}_h, \mathbf{0}) \in V_h$, and using from the definition of \mathcal{A}^K (cf. (3.7)) that

$$\mathcal{A}^K(\mathbf{r}, \zeta \pm \tilde{\zeta}) = \mathcal{A}^K(\mathbf{r}, \zeta) \pm \mathcal{A}^K(\mathbf{0}, \tilde{\zeta}) \quad \forall \mathbf{r} \in X^K, \quad \forall \zeta, \tilde{\zeta} \in H^K,$$

we find that

$$\begin{aligned} \alpha \|(\delta_h^{\mathbf{t}}, \delta_h^\sigma)\|_{X \times H}^2 &\leq [\mathcal{A}_h(\mathcal{P}_X^h(\mathbf{t}), \Pi^h(\sigma) - \sigma_h) - \mathcal{A}_h(\mathbf{t}_h, \mathbf{0}), (\delta_h^{\mathbf{t}}, \delta_h^\sigma)] \\ &= [\mathcal{A}_h(\mathcal{P}_X^h(\mathbf{t}), \Pi^h(\sigma)) - \mathcal{A}_h(\mathbf{0}, \sigma_h) - \mathcal{A}_h(\mathbf{t}_h, \mathbf{0}), (\delta_h^{\mathbf{t}}, \delta_h^\sigma)] \\ &= [\mathcal{A}_h(\mathcal{P}_X^h(\mathbf{t}), \Pi^h(\sigma)), (\delta_h^{\mathbf{t}}, \delta_h^\sigma)] - [\mathcal{A}_h(\mathbf{t}_h, \sigma_h), (\delta_h^{\mathbf{t}}, \delta_h^\sigma)], \end{aligned}$$

which, noting from the first equations of (2.6) and (3.12) that

$$[\mathcal{A}_h(\mathbf{t}_h, \sigma_h), (\mathbf{s}_h, \tau_h)] = [\mathcal{A}(\mathbf{t}, \sigma), (\mathbf{s}_h, \tau_h)] \quad \forall (\mathbf{s}_h, \tau_h) \in V_h,$$

in particular for $(\mathbf{s}_h, \tau_h) = (\delta_h^{\mathbf{t}}, \delta_h^\sigma)$, and adding and subtracting $[\mathcal{A}_h(\mathcal{P}_X^h(\mathbf{t}), \widehat{\Pi}^h(\sigma)), (\delta_h^{\mathbf{t}}, \delta_h^\sigma)]$, yields

$$\begin{aligned} \alpha \|(\delta_h^{\mathbf{t}}, \delta_h^\sigma)\|_{X \times H}^2 &\leq [\mathcal{A}_h(\mathcal{P}_X^h(\mathbf{t}), \Pi^h(\sigma)), (\delta_h^{\mathbf{t}}, \delta_h^\sigma)] - [\mathcal{A}(\mathbf{t}, \sigma), (\delta_h^{\mathbf{t}}, \delta_h^\sigma)] \\ &= [\mathcal{A}_h(\mathcal{P}_X^h(\mathbf{t}), \Pi^h(\sigma)) - \mathcal{A}_h(\mathcal{P}_X^h(\mathbf{t}), \widehat{\Pi}^h(\sigma)), (\delta_h^{\mathbf{t}}, \delta_h^\sigma)] \\ &\quad + [\mathcal{A}_h(\mathcal{P}_X^h(\mathbf{t}), \widehat{\Pi}^h(\sigma)) - \mathcal{A}(\mathbf{t}, \sigma), (\delta_h^{\mathbf{t}}, \delta_h^\sigma)]. \end{aligned} \tag{3.26}$$

The two expressions on the right-hand side of (3.26) are bounded in what follows. Indeed, employing (3.18), the boundedness of $\widehat{\Pi}^h$ (cf. (3.8)), and the fact that $\widehat{\Pi}^h$ is a projection (i.e. $\widehat{\Pi}^h \widehat{\Pi}^h = \widehat{\Pi}^h$), we first deduce that

$$\begin{aligned} &[\mathcal{A}_h(\mathcal{P}_X^h(\mathbf{t}), \Pi^h(\sigma)) - \mathcal{A}_h(\mathcal{P}_X^h(\mathbf{t}), \widehat{\Pi}^h(\sigma)), (\delta_h^{\mathbf{t}}, \delta_h^\sigma)] \\ &\leq C \left\{ \|\widehat{\Pi}^h\{\sigma - \Pi^h(\sigma)\}\|_{0, \Omega} + \|\Pi^h(\sigma) - \widehat{\Pi}^h\{\Pi^h(\sigma)\}\|_{0, \Omega} \right\} \|(\delta_h^{\mathbf{t}}, \delta_h^\sigma)\|_{X \times H}. \end{aligned} \tag{3.27}$$

At the same time, using the definitions of \mathcal{A} (cf. (2.11)) and \mathcal{A}_h (cf. (3.11)), it is easy to check that

$$\begin{aligned} &[\mathcal{A}_h(\mathcal{P}_X^h(\mathbf{t}), \widehat{\Pi}^h(\sigma)) - \mathcal{A}(\mathbf{t}, \sigma), (\delta_h^{\mathbf{t}}, \delta_h^\sigma)] = [\mathbf{A}(\mathcal{P}_X^h(\mathbf{t})) - \mathbf{A}(\mathbf{t}), \delta_h^{\mathbf{t}}] \\ &\quad + \int_{\Omega} (\sigma - \widehat{\Pi}^h(\sigma)) : \delta_h^{\mathbf{t}} - \int_{\Omega} \mathbf{t} : \delta_h^\sigma + \int_{\Omega} \mathcal{P}_X^h(\mathbf{t}) : \widehat{\Pi}^h(\delta_h^\sigma) \\ &\quad - \kappa \int_{\Omega} (\mathbf{A}(\mathcal{P}_X^h(\mathbf{t})) - (\widehat{\Pi}^h(\sigma))^{\mathbf{d}}) : \widehat{\Pi}^h(\delta_h^\sigma)^{\mathbf{d}} - \kappa \int_{\Omega} (\sigma^{\mathbf{d}} - 2\mu(|\mathbf{t}|)\mathbf{t}) : (\delta_h^\sigma)^{\mathbf{d}}. \end{aligned} \tag{3.28}$$

On the other hand, it follows from the first identity of (2.2) that $\|2\mu(|\mathbf{t}|)\mathbf{t}\|_{0, \Omega} \leq 4\gamma_0 \|\mathbf{t}\|_{0, \Omega}$, which, along with the fact that $\text{tr}(2\mu(|\mathbf{t}|)\mathbf{t}) = 0$, implies that $2\mu(|\mathbf{t}|)\mathbf{t} \in X$. Thus, taking the test vector $(\mathbf{s}, \tau) := (\sigma^{\mathbf{d}} - 2\mu(|\mathbf{t}|)\mathbf{t}, \mathbf{0}) \in X \times H$ in the first equation of (2.6), we obtain that

$$\sigma^{\mathbf{d}} - 2\mu(|\mathbf{t}|)\mathbf{t} = \mathbf{0} \quad \text{in } \Omega, \tag{3.29}$$

whence, using additionally from (3.9) that $\int_{\Omega} \mathcal{P}_X^h(\mathbf{t}) : \widehat{\Pi}^h(\delta_h^\sigma) = \int_{\Omega} \mathcal{P}_X^h(\mathbf{t}) : \delta_h^\sigma$, and adding and subtracting $\mathbf{A}(\mathbf{t}) := 2\mu(|\mathbf{t}|)\mathbf{t} = \sigma^{\mathbf{d}}$ in the remaining term of the last row of (3.28), this latter equation becomes

$$\begin{aligned} &[\mathcal{A}_h(\mathcal{P}_X^h(\mathbf{t}), \widehat{\Pi}^h(\sigma)) - \mathcal{A}(\mathbf{t}, \sigma), (\delta_h^{\mathbf{t}}, \delta_h^\sigma)] = [\mathbf{A}(\mathcal{P}_X^h(\mathbf{t})) - \mathbf{A}(\mathbf{t}), \delta_h^{\mathbf{t}} - \kappa(\widehat{\Pi}^h(\delta_h^\sigma))^{\mathbf{d}}] \\ &\quad + \int_{\Omega} (\sigma - \widehat{\Pi}^h(\sigma)) : \delta_h^{\mathbf{t}} - \int_{\Omega} (\mathbf{t} - \mathcal{P}_X^h(\mathbf{t})) : \delta_h^\sigma - \kappa \int_{\Omega} (\sigma - \widehat{\Pi}^h(\sigma))^{\mathbf{d}} : (\widehat{\Pi}^h(\delta_h^\sigma))^{\mathbf{d}}. \end{aligned}$$

Now, applying the Cauchy-Schwarz inequality, the Lipschitz-continuity of \mathbf{A} (cf. (2.13)), and the boundedness of $\widehat{\Pi}^h$ (cf. (3.8)), we arrive at

$$[\mathcal{A}_h(\mathcal{P}_X^h(\mathbf{t}), \widehat{\Pi}^h(\boldsymbol{\sigma})) - \mathcal{A}(\mathbf{t}, \boldsymbol{\sigma}), (\boldsymbol{\delta}_h^{\mathbf{t}}, \boldsymbol{\delta}_h^{\boldsymbol{\sigma}})] \leq C \left\{ \|\mathbf{t} - \mathcal{P}_X^h(\mathbf{t})\|_{0,\Omega} + \|\boldsymbol{\sigma} - \widehat{\Pi}^h(\boldsymbol{\sigma})\|_{0,\Omega} \right\} \|(\boldsymbol{\delta}_h^{\mathbf{t}}, \boldsymbol{\delta}_h^{\boldsymbol{\sigma}})\|_{X \times H},$$

which, along with (3.26) and (3.27), imply

$$\begin{aligned} \|\boldsymbol{\delta}_h^{\mathbf{t}}\|_{0,\Omega} + \|\boldsymbol{\delta}_h^{\boldsymbol{\sigma}}\|_{\mathbf{div};\Omega} &\leq C \left\{ \|\mathbf{t} - \mathcal{P}_X^h(\mathbf{t})\|_{0,\Omega} + \|\boldsymbol{\sigma} - \widehat{\Pi}^h(\boldsymbol{\sigma})\|_{0,\Omega} \right. \\ &\quad \left. + \|\widehat{\Pi}^h\{\boldsymbol{\sigma} - \Pi^h(\boldsymbol{\sigma})\}\|_{0,\Omega} + \|\Pi^h(\boldsymbol{\sigma}) - \widehat{\Pi}^h\{\Pi^h(\boldsymbol{\sigma})\}\|_{0,\Omega} \right\}. \end{aligned} \quad (3.30)$$

It remains to bound the last two terms in the foregoing inequality. In fact, adding and subtracting $\boldsymbol{\sigma} - \widehat{\Pi}^h(\boldsymbol{\sigma})$, we get for the second expression

$$\|\Pi^h(\boldsymbol{\sigma}) - \widehat{\Pi}^h\{\Pi^h(\boldsymbol{\sigma})\}\|_{0,\Omega} \leq \|\boldsymbol{\sigma} - \Pi^h(\boldsymbol{\sigma})\|_{0,\Omega} + \|\boldsymbol{\sigma} - \widehat{\Pi}^h(\boldsymbol{\sigma})\|_{0,\Omega} + \|\widehat{\Pi}^h\{\boldsymbol{\sigma} - \Pi^h(\boldsymbol{\sigma})\}\|_{0,\Omega}. \quad (3.31)$$

In turn, employing once again the boundedness of $\widehat{\Pi}^h$ (cf. (3.8)), it follows that

$$\|\widehat{\Pi}^h\{\boldsymbol{\sigma} - \Pi^h(\boldsymbol{\sigma})\}\|_{0,\Omega} \leq \widehat{c}_1 \|\boldsymbol{\sigma} - \Pi^h(\boldsymbol{\sigma})\|_{0,\Omega} + \widehat{c}_2 h \|\mathbf{div}(\boldsymbol{\sigma} - \Pi^h(\boldsymbol{\sigma}))\|_{0,\Omega},$$

which, using (3.22) and the fact that $\mathbf{div}(\boldsymbol{\sigma}) = -\mathbf{f}$, gives

$$\|\widehat{\Pi}^h\{\boldsymbol{\sigma} - \Pi^h(\boldsymbol{\sigma})\}\|_{0,\Omega} \leq \widehat{c}_1 \|\boldsymbol{\sigma} - \Pi^h(\boldsymbol{\sigma})\|_{0,\Omega} + \widehat{c}_2 h \|\mathbf{f} - \mathcal{P}_Y^h(\mathbf{f})\|_{0,\Omega}. \quad (3.32)$$

In this way, replacing (3.31) and (3.32) into (3.30), and then the resulting estimate back into (3.25), and finally observing from (2.5) and (3.13) that there holds

$$\|p - p_h\|_{0,\Omega} = \frac{1}{2} \|\mathrm{tr}(\boldsymbol{\sigma}) - \mathrm{tr}(\boldsymbol{\sigma}_h)\|_{0,\Omega} \leq \frac{1}{\sqrt{2}} \|\boldsymbol{\sigma} - \boldsymbol{\sigma}_h\|_{0,\Omega},$$

we conclude (3.23) and finish the proof of the theorem. \square

The *a priori* error analysis is continued now with the estimate for $\|\mathbf{u} - \mathbf{u}_h\|_{0,\Omega}$.

Theorem 3.3. *Let $((\mathbf{t}, \boldsymbol{\sigma}), \mathbf{u}) \in (X \times H) \times Y$ and $((\mathbf{t}_h, \boldsymbol{\sigma}_h), \mathbf{u}_h) \in (X_h \times H_h) \times Y_h$ be the unique solutions of the continuous and discrete schemes (2.6) and (3.12), respectively, and assume that $\boldsymbol{\sigma} \in \widetilde{\mathbb{H}}(\Omega)$. Then, there exist $C > 0$, independent of h , such that*

$$\begin{aligned} \|\mathbf{u} - \mathbf{u}_h\|_{0,\Omega} &\leq C \left\{ \|\mathbf{t} - \mathcal{P}_X^h(\mathbf{t})\|_{0,\Omega} + \|\boldsymbol{\sigma} - \Pi^h(\boldsymbol{\sigma})\|_{0,\Omega} \right. \\ &\quad \left. + \|\boldsymbol{\sigma} - \widehat{\Pi}^h(\boldsymbol{\sigma})\|_{0,\Omega} + \|\mathbf{u} - \mathcal{P}_Y^h(\mathbf{u})\|_{0,\Omega} + h \|\mathbf{f} - \mathcal{P}_Y^h(\mathbf{f})\|_{0,\Omega} \right\}. \end{aligned} \quad (3.33)$$

Proof. Our starting point is again the triangle inequality, thanks to which we obtain

$$\|\mathbf{u} - \mathbf{u}_h\|_{0,\Omega} \leq \|\mathbf{u} - \mathcal{P}_Y^h(\mathbf{u})\|_{0,\Omega} + \|\boldsymbol{\delta}_h^{\mathbf{u}}\|_{0,\Omega}, \quad (3.34)$$

where $\boldsymbol{\delta}_h^{\mathbf{u}} := \mathcal{P}_Y^h(\mathbf{u}) - \mathbf{u}_h \in Y_h$. Next, a straightforward application of the discrete inf-sup condition for \mathcal{B} (cf. Lemma 3.4) gives

$$\|\boldsymbol{\delta}_h^{\mathbf{u}}\|_{0,\Omega} \leq \frac{1}{\beta} \sup_{\substack{(\mathbf{s}_h, \boldsymbol{\tau}_h) \in X_h \times H_h \\ (\mathbf{s}_h, \boldsymbol{\tau}_h) \neq \mathbf{0}}} \frac{[\mathcal{B}(\mathbf{s}_h, \boldsymbol{\tau}_h), \boldsymbol{\delta}_h^{\mathbf{u}}]}{\|(\mathbf{s}_h, \boldsymbol{\tau}_h)\|_{X \times H}}, \quad (3.35)$$

where, according to the definition of \mathcal{B} (cf. (2.8)), and recalling that $\mathcal{P}_Y^h : \mathbf{L}^2(\Omega) \rightarrow Y_h$ is the $\mathbf{L}^2(\Omega)$ -orthogonal projector, and that $\mathbf{div}(\boldsymbol{\tau}_h) \in Y_h$ (cf. (A.3)), there holds

$$[\mathcal{B}(\mathbf{s}_h, \boldsymbol{\tau}_h), \boldsymbol{\delta}_h^{\mathbf{u}}] = \int_{\Omega} \mathcal{P}_Y^h(\mathbf{u}) \cdot \mathbf{div}(\boldsymbol{\tau}_h) - \int_{\Omega} \mathbf{u}_h \cdot \mathbf{div}(\boldsymbol{\tau}_h) = [\mathcal{B}(\mathbf{0}, \boldsymbol{\tau}_h), \mathbf{u}] - [\mathcal{B}(\mathbf{0}, \boldsymbol{\tau}_h), \mathbf{u}_h].$$

Then, applying the first equations of (2.6) and (3.12), and adding and subtracting $\mathcal{A}_h(\mathbf{t}_h, \widehat{\Pi}^h(\boldsymbol{\sigma}))$, it follows that

$$\begin{aligned} [\mathcal{B}(\mathbf{s}_h, \boldsymbol{\tau}_h), \boldsymbol{\delta}_h^{\mathbf{u}}] &= [\mathcal{A}_h(\mathbf{t}_h, \boldsymbol{\sigma}_h), (\mathbf{0}, \boldsymbol{\tau}_h)] - [\mathcal{A}(\mathbf{t}, \boldsymbol{\sigma}), (\mathbf{0}, \boldsymbol{\tau}_h)] \\ &= [\mathcal{A}_h(\mathbf{t}_h, \boldsymbol{\sigma}_h) - \mathcal{A}_h(\mathbf{t}_h, \widehat{\Pi}^h(\boldsymbol{\sigma})), (\mathbf{0}, \boldsymbol{\tau}_h)] + [\mathcal{A}_h(\mathbf{t}_h, \widehat{\Pi}^h(\boldsymbol{\sigma})) - \mathcal{A}(\mathbf{t}, \boldsymbol{\sigma}), (\mathbf{0}, \boldsymbol{\tau}_h)], \end{aligned} \quad (3.36)$$

so that we now proceed to bound the two expressions on the right-hand side of (3.36). In fact, employing the incomplete Lipschitz-continuity estimate (3.18), the fact that clearly $(\mathbf{I} - \widehat{\Pi}^h)\widehat{\Pi}^h(\boldsymbol{\sigma})$ is the null operator, and the boundedness of $\widehat{\Pi}^h$ (cf. (3.8)), we first obtain that

$$\begin{aligned} &|[\mathcal{A}_h(\mathbf{t}_h, \boldsymbol{\sigma}_h) - \mathcal{A}_h(\mathbf{t}_h, \widehat{\Pi}^h(\boldsymbol{\sigma})), (\mathbf{0}, \boldsymbol{\tau}_h)]| \\ &\leq C \left\{ \|\widehat{\Pi}^h(\boldsymbol{\sigma} - \boldsymbol{\sigma}_h)\|_{0,\Omega} + \|\boldsymbol{\sigma}_h - \widehat{\Pi}^h(\boldsymbol{\sigma}_h)\|_{0,\Omega} \right\} \|\boldsymbol{\tau}_h\|_{\mathbf{div};\Omega}. \end{aligned} \quad (3.37)$$

In turn, bearing in mind again the definitions of \mathcal{A} (cf. (2.11)) and \mathcal{A}_h (cf. (3.11)), and utilizing the identities (3.9) and (3.29), we find that

$$\begin{aligned} &[\mathcal{A}_h(\mathbf{t}_h, \widehat{\Pi}^h(\boldsymbol{\sigma})) - \mathcal{A}(\mathbf{t}, \boldsymbol{\sigma}), (\mathbf{0}, \boldsymbol{\tau}_h)] = \kappa[\mathbf{A}(\mathbf{t}) - \mathbf{A}(\mathbf{t}_h), (\widehat{\Pi}^h(\boldsymbol{\tau}_h))^{\mathbf{d}}] \\ &\quad - \int_{\Omega} (\mathbf{t} - \mathbf{t}_h) : \boldsymbol{\tau}_h - \kappa \int_{\Omega} (\boldsymbol{\sigma} - \widehat{\Pi}^h(\boldsymbol{\sigma}))^{\mathbf{d}} : (\widehat{\Pi}^h(\boldsymbol{\tau}_h))^{\mathbf{d}}, \end{aligned}$$

from which, applying the Cauchy-Schwarz inequality, the Lipschitz-continuity of \mathbf{A} (cf. (2.13)), and the boundedness of $\widehat{\Pi}^h$ (cf. (3.8)), we arrive at

$$|[\mathcal{A}_h(\mathbf{t}_h, \widehat{\Pi}^h(\boldsymbol{\sigma})) - \mathcal{A}(\mathbf{t}, \boldsymbol{\sigma}), (\mathbf{0}, \boldsymbol{\tau}_h)]| \leq C \left\{ \|\mathbf{t} - \mathbf{t}_h\|_{0,\Omega} + \|\boldsymbol{\sigma} - \widehat{\Pi}^h(\boldsymbol{\sigma})\|_{0,\Omega} \right\} \|\boldsymbol{\tau}_h\|_{\mathbf{div};\Omega}. \quad (3.38)$$

Hence, employing (3.37) and (3.38) to derive an upper bound for $|[\mathcal{B}(\mathbf{s}_h, \boldsymbol{\tau}_h), \boldsymbol{\delta}_h^{\mathbf{u}}]|$ (cf. (3.36)), and replacing the resulting estimate back into (3.35), we deduce that

$$\|\boldsymbol{\delta}_h^{\mathbf{u}}\|_{0,\Omega} \leq C \left\{ \|\mathbf{t} - \mathbf{t}_h\|_{0,\Omega} + \|\boldsymbol{\sigma} - \widehat{\Pi}^h(\boldsymbol{\sigma})\|_{0,\Omega} + \|\widehat{\Pi}^h(\boldsymbol{\sigma} - \boldsymbol{\sigma}_h)\|_{0,\Omega} + \|\boldsymbol{\sigma}_h - \widehat{\Pi}^h(\boldsymbol{\sigma}_h)\|_{0,\Omega} \right\}. \quad (3.39)$$

In addition, adding and subtracting $\boldsymbol{\sigma} - \widehat{\Pi}^h(\boldsymbol{\sigma})$, we readily obtain that

$$\|\boldsymbol{\sigma}_h - \widehat{\Pi}^h(\boldsymbol{\sigma}_h)\|_{0,\Omega} \leq \|\boldsymbol{\sigma} - \boldsymbol{\sigma}_h\|_{0,\Omega} + \|\boldsymbol{\sigma} - \widehat{\Pi}^h(\boldsymbol{\sigma})\|_{0,\Omega} + \|\widehat{\Pi}^h(\boldsymbol{\sigma} - \boldsymbol{\sigma}_h)\|_{0,\Omega}, \quad (3.40)$$

whereas, using again the boundedness of $\widehat{\Pi}^h$ (cf. (3.8)) and (3.24), it follows that

$$\begin{aligned} \|\widehat{\Pi}^h(\boldsymbol{\sigma} - \boldsymbol{\sigma}_h)\|_{0,\Omega} &\leq \widehat{c}_1 \|\boldsymbol{\sigma} - \boldsymbol{\sigma}_h\|_{0,\Omega} + \widehat{c}_2 h \|\mathbf{div}(\boldsymbol{\sigma} - \boldsymbol{\sigma}_h)\|_{0,\Omega} \\ &= \widehat{c}_1 \|\boldsymbol{\sigma} - \boldsymbol{\sigma}_h\|_{0,\Omega} + \widehat{c}_2 h \|\mathbf{f} - \mathcal{P}_Y^h(\mathbf{f})\|_{0,\Omega}. \end{aligned} \quad (3.41)$$

In this way, using (3.40) and (3.41) to control the last two expressions in (3.39), replacing the resulting estimate back into (3.34), and finally employing (3.23) to bound $\|\mathbf{t} - \mathbf{t}_h\|_{0,\Omega} + \|\boldsymbol{\sigma} - \boldsymbol{\sigma}_h\|_{0,\Omega}$, we conclude (3.33) and end the proof of the theorem. \square

3.5 Computable approximations of $\boldsymbol{\sigma}$ and p

We now introduce the fully computable approximations of $\boldsymbol{\sigma}$ and p given by

$$\widehat{\boldsymbol{\sigma}}_h := \widehat{\Pi}^h(\boldsymbol{\sigma}_h) \quad \text{and} \quad \widehat{p}_h := -\frac{1}{2} \text{tr}(\widehat{\boldsymbol{\sigma}}_h), \quad (3.42)$$

and establish next the corresponding *a priori* error estimates.

Theorem 3.4. *There exists a positive constant C , independent of h , such that*

$$\begin{aligned} \|\boldsymbol{\sigma} - \widehat{\boldsymbol{\sigma}}_h\|_{0,\Omega} + \|p - \widehat{p}_h\|_{0,\Omega} &\leq C \left\{ \|\mathbf{t} - \mathcal{P}_X^h(\mathbf{t})\|_{0,\Omega} + \|\boldsymbol{\sigma} - \Pi^h(\boldsymbol{\sigma})\|_{0,\Omega} \right. \\ &\quad \left. + \|\boldsymbol{\sigma} - \widehat{\Pi}^h(\boldsymbol{\sigma})\|_{0,\Omega} + h \|\mathbf{f} - \mathcal{P}_Y^h(\mathbf{f})\|_{0,\Omega} \right\}. \end{aligned} \quad (3.43)$$

Proof. We begin by noticing from (2.5) and (3.42) that

$$\|p - \widehat{p}_h\|_{0,\Omega} = \frac{1}{2} \|\text{tr}(\boldsymbol{\sigma} - \widehat{\boldsymbol{\sigma}}_h)\|_{0,\Omega} \leq \frac{1}{\sqrt{2}} \|\boldsymbol{\sigma} - \widehat{\boldsymbol{\sigma}}_h\|_{0,\Omega},$$

which certainly yields

$$\|\boldsymbol{\sigma} - \widehat{\boldsymbol{\sigma}}_h\|_{0,\Omega} + \|p - \widehat{p}_h\|_{0,\Omega} \leq \left(1 + \frac{1}{\sqrt{2}}\right) \|\boldsymbol{\sigma} - \widehat{\boldsymbol{\sigma}}_h\|_{0,\Omega}. \quad (3.44)$$

Then, adding and subtracting $\boldsymbol{\sigma}_h$, we get

$$\|\boldsymbol{\sigma} - \widehat{\boldsymbol{\sigma}}_h\|_{0,\Omega} \leq \|\boldsymbol{\sigma} - \boldsymbol{\sigma}_h\|_{0,\Omega} + \|\boldsymbol{\sigma}_h - \widehat{\Pi}^h(\boldsymbol{\sigma}_h)\|_{0,\Omega},$$

which, together with (3.40), (3.41), (3.44), and the estimate for $\|\boldsymbol{\sigma} - \boldsymbol{\sigma}_h\|_{0,\Omega}$ provided by (3.23), lead to (3.43) and complete the proof. \square

4 A particular mixed-VEM scheme

We now proceed to define particular choices for the local subspaces X^K , H^K and Y^K , which satisfy (A.1)-(A.5) for each $K \in \mathcal{T}_h$ and (A.6). In addition, polynomial subspaces \widehat{H}^K of $\mathbb{H}(\mathbf{div}; K)$, and associated projectors $\widehat{\Pi}^K : \mathbb{H}(\mathbf{div}; K) \rightarrow \widehat{H}^K$ verifying the assumptions (P.1)-(P.3), are also introduced in what follows.

4.1 A first choice

This choice is motivated by the linear version of our problem (2.1), which was analyzed recently in [12]. More precisely, given an integer $k \geq 1$, we set

$$\begin{aligned} X^K &:= \left\{ \nabla \text{curl}(q) : q \in \text{span}\{\mathbf{x}^\alpha : 2 \leq |\alpha| \leq k+2\} \subseteq \mathbf{P}_{k+2}(K) \right\}, \\ H^K &:= \left\{ \boldsymbol{\tau} \in \mathbb{H}(\mathbf{div}; K) \cap \mathbb{H}(\mathbf{rot}; K) : \boldsymbol{\tau} \mathbf{n}|_e \in \mathbf{P}_k(e) \quad \forall \text{ edge } e \in \partial K, \right. \\ &\quad \left. \text{div}(\boldsymbol{\tau}) \in \mathbf{P}_{k-1}(K), \quad \text{and} \quad \mathbf{rot}(\boldsymbol{\tau}) \in \mathbf{P}_{k-1}(K) \right\}, \\ Y^K &:= \mathbf{P}_{k-1}(K), \end{aligned} \quad (4.1)$$

where $\mathbf{curl}(q) := (\partial_{x_2}q, -\partial_{x_1}q)^\dagger$, and $\mathbf{rot}(\boldsymbol{\tau}) := (\partial_{x_1}\tau_{12} - \partial_{x_2}\tau_{11}, \partial_{x_1}\tau_{22} - \partial_{x_2}\tau_{21})^\dagger$. Then, we notice from (4.1) that the assumptions **(A.1)**, **(A.2)**, and **(A.3)** are trivially satisfied. In turn, **(A.4)** is established in [12, Lemmas 3.1 and 4.5] (see also [9]), whereas **(A.5)** and **(A.6)** follow from the analysis provided in [12, Section 3.3]. In fact, it suffices to define (cf. [12, eq. (3.12)])

$$\tilde{\mathbb{H}}(K) := \left\{ \boldsymbol{\tau} \in \mathbb{H}(\mathbf{div}; K) : \boldsymbol{\tau} \in \mathbb{L}^s(K) \quad (\text{for some } s > 2), \quad \mathbf{rot}(\boldsymbol{\tau}) \in \mathbb{L}^1(K) \right\} \quad \forall K \in \mathcal{T}_h,$$

$$\tilde{\mathbb{H}}(\Omega) := \left\{ \boldsymbol{\tau} \in \mathbb{H}(\mathbf{div}; \Omega) : \boldsymbol{\tau}|_K \in \tilde{\mathbb{H}}(K) \quad \forall K \in \mathcal{T}_h \right\},$$

$$\Pi^h := \Pi_k^h, \quad \text{and} \quad \Pi^K := \Pi_k^K,$$

where Π_k^h and Π_k^K are the global and local interpolation operators whose corresponding degrees of freedom are given by [12, eq. (3.13)] and [12, eq. (3.16)], respectively. In addition, note that in this case the identity (3.6) in **(A.5)** corresponds to [12, eq. (3.14)]. Alternatively, and because of the continuous imbedding of \mathbb{H}^1 into \mathbb{L}^4 , we could proceed as in [13, Section 3.4] and, instead of the foregoing definitions, simply set

$$\tilde{\mathbb{H}}(K) := \mathbb{H}^1(K) \quad \forall K \in \mathcal{T}_h \quad \text{and} \quad \tilde{\mathbb{H}}(\Omega) := \left\{ \boldsymbol{\tau} \in \mathbb{H}(\mathbf{div}; \Omega) : \boldsymbol{\tau}|_K \in \mathbb{H}^1(K) \quad \forall K \in \mathcal{T}_h \right\}. \quad (4.2)$$

Next, following [12, Section 4], we define

$$\hat{H}^K := X^K \oplus \mathbb{P}_k(K)\mathbb{I},$$

and introduce the local projection $\hat{\Pi}^K : \mathbb{H}(\mathbf{div}; K) \rightarrow \hat{H}^K$ defined in terms of the decomposition:

$$\hat{\Pi}^K(\boldsymbol{\zeta}) := \hat{\boldsymbol{\zeta}}_\nabla + q_\boldsymbol{\zeta}\mathbb{I} + c_\boldsymbol{\zeta}\mathbb{I} \in \hat{H}^K \quad \forall \boldsymbol{\zeta} \in \mathbb{H}(\mathbf{div}; K), \quad (4.3)$$

where the components $\hat{\boldsymbol{\zeta}}_\nabla \in X^K$, $q_\boldsymbol{\zeta} \in \hat{\mathbb{P}}_k(K) := \text{span}\{\mathbf{x}^\alpha : 1 \leq |\alpha| \leq k\}$, and $c_\boldsymbol{\zeta} \in \mathbb{R}$ are computed according to the following sequentially connected problems:

- Find $\hat{\boldsymbol{\zeta}}_\nabla \in X^K$ such that

$$\int_K \hat{\boldsymbol{\zeta}}_\nabla : \boldsymbol{\tau} = \int_K \boldsymbol{\zeta} : \boldsymbol{\tau} \quad \forall \boldsymbol{\tau} \in X^K, \quad (4.4)$$

- Find $q_\boldsymbol{\zeta} \in \hat{\mathbb{P}}_k(K)$ such that

$$\int_K \mathbf{div}(q_\boldsymbol{\zeta}\mathbb{I}) \cdot \mathbf{div}(q\mathbb{I}) = \int_K \mathbf{div}(\boldsymbol{\zeta} - \hat{\boldsymbol{\zeta}}_\nabla) \cdot \mathbf{div}(q\mathbb{I}) \quad \forall q \in \hat{\mathbb{P}}_k(K), \quad (4.5)$$

- Find $c_\boldsymbol{\zeta} \in \mathbb{R}$ such that

$$\int_K \text{tr}(\hat{\Pi}^K(\boldsymbol{\zeta})) = \int_K \text{tr}(\boldsymbol{\zeta}),$$

which, establishes that

$$c_\boldsymbol{\zeta} = \frac{1}{2|K|} \int_K \{\text{tr}(\boldsymbol{\zeta}) - 2q_\boldsymbol{\zeta}\}. \quad (4.6)$$

It is not difficult to check (see [12, Section 4] for details) that $\hat{\Pi}^K$, defined by (4.3) - (4.6), is in fact a projector and verifies the properties **(P.1)**, **(P.2)** and **(P.3)**. In particular, it is shown in [12, Lemma 4.2] that (3.8) in **(P.2)** is satisfied with $\hat{c}_1 = \hat{c}_2 > 0$. In addition, it is clear, thanks to the definition of X^K (cf. (4.1)) and the identity (4.4), that there holds (3.9) in **(P.3)**.

Hence, as a straightforward consequence of Theorem 3.1 and the foregoing discussion, we are able to state the following result.

Theorem 4.1. *Let X^K , H^K and Y^K be those described in (4.1), and let $\widehat{\Pi}^K$ as defined by (4.3) - (4.6). In addition, assume that the parameter κ lies in $\left(0, \frac{\alpha_0}{\gamma_0}\right)$, where γ_0 and α_0 are the positive constants from (2.2) and (2.3), respectively. Then the Galerkin scheme (3.12) has a unique solution $((\mathbf{t}_h, \boldsymbol{\sigma}_h), \mathbf{u}_h) \in (X_h \times H_h) \times Y_h$ and there exists a constant $C > 0$, independent of h , such that*

$$\|\mathbf{t}_h\|_{0,\Omega} + \|\boldsymbol{\sigma}_h\|_{\text{div};\Omega} + \|\mathbf{u}_h\|_{0,\Omega} \leq C \left\{ \|\mathbf{f}\|_{0,\Omega} + \|\mathbf{g}\|_{1/2,\Gamma} \right\}.$$

Moreover, a direct application now of Theorems 3.2, 3.3, and 3.4 yields the existence of a constant $C > 0$, independent of h , such that

$$\begin{aligned} & \|\mathbf{t} - \mathbf{t}_h\|_{0,\Omega} + \|\boldsymbol{\sigma} - \boldsymbol{\sigma}_h\|_{0,\Omega} + \|p - p_h\|_{0,\Omega} + \|\boldsymbol{\sigma} - \widehat{\boldsymbol{\sigma}}_h\|_{0,\Omega} + \|p - \widehat{p}_h\|_{0,\Omega} \\ & \leq C \sum_{K \in \mathcal{T}_h} \left\{ \|\mathbf{t} - \mathcal{P}_{k,\nabla}^K(\mathbf{t})\|_{0,K} + \|\boldsymbol{\sigma} - \Pi^K(\boldsymbol{\sigma})\|_{0,K} + \|\boldsymbol{\sigma} - \widehat{\Pi}^K(\boldsymbol{\sigma})\|_{0,K} + h_K \|\mathbf{f} - \mathcal{P}_{k-1}^K(\mathbf{f})\|_{0,K} \right\}, \end{aligned}$$

and

$$\begin{aligned} \|\mathbf{u} - \mathbf{u}_h\|_{0,\Omega} & \leq C \sum_{K \in \mathcal{T}_h} \left\{ \|\mathbf{t} - \mathcal{P}_{k,\nabla}^K(\mathbf{t})\|_{0,K} + \|\boldsymbol{\sigma} - \Pi^K(\boldsymbol{\sigma})\|_{0,K} + \|\boldsymbol{\sigma} - \widehat{\Pi}^K(\boldsymbol{\sigma})\|_{0,K} \right. \\ & \quad \left. + h_K \|\mathbf{f} - \mathcal{P}_{k-1}^K(\mathbf{f})\|_{0,K} + \|\mathbf{u} - \mathcal{P}_{k-1}^K(\mathbf{u})\|_{0,K} \right\}, \end{aligned}$$

where $\mathcal{P}_{k,\nabla}^K : \mathbb{L}^2(K) \rightarrow X^K$ and $\mathcal{P}_{k-1}^K : \mathbb{L}^2(K) \rightarrow Y^k$ denote the corresponding orthogonal projections. In particular, note from (4.4) that $\mathcal{P}_{k,\nabla}^K(\boldsymbol{\zeta}) = \widehat{\boldsymbol{\zeta}}_{\nabla} \quad \forall \boldsymbol{\zeta} \in \mathbb{H}(\text{div}; K)$. In this way, since $\mathbf{t} = \nabla \mathbf{u}$, and $\text{tr}(\mathbf{t}) = 0$ (which is equivalent to the fact that \mathbf{u} is divergence free), we can write

$$\mathbf{t}^{\text{d}} = \mathbf{t} = \nabla \text{curl}(w) \quad \text{for some } w \in \mathbb{H}^2(\Omega),$$

whence, under additional regularity assumptions on w , the approximation property provided by [12, Lemma 4.4] can be applied to \mathbf{t} . More precisely, if $w|_K \in \mathbb{H}^{r+2}(K)$, with $1 \leq r \leq k+1$, there holds

$$\|\mathbf{t} - \widehat{\Pi}^K(\mathbf{t})\|_{0,K} \leq C h_K^r |\mathbf{t}|_{r,K},$$

and thus

$$\|\mathbf{t} - \mathcal{P}_{k,\nabla}^K(\mathbf{t})\|_{0,K} = \|\mathbf{t} - \widehat{\mathbf{t}}_{\nabla}\|_{0,K} \leq \|\mathbf{t} - \widehat{\Pi}^K(\mathbf{t})\|_{0,K} \leq C h_K^r |\mathbf{t}|_{r,K}.$$

In turn, we know from [12, Lemma 3.6] (cf. [9, eq. (4.8)]) that when $\boldsymbol{\sigma}|_K \in \mathbb{H}^r(K)$, with $1 \leq r \leq k+1$, one obtains that

$$\|\boldsymbol{\sigma} - \Pi^K(\boldsymbol{\sigma})\|_{0,K} \leq C h_K^r |\boldsymbol{\sigma}|_{r,K},$$

whereas [12, Lemma 3.4] establishes that when $\mathbf{u}|_K, \mathbf{f}|_K \in \mathbb{H}^r(K)$, with $1 \leq r \leq k$, there hold

$$\|\mathbf{u} - \mathcal{P}_{k-1}^K(\mathbf{u})\|_{0,K} \leq C h_K^r |\mathbf{u}|_{r,K} \quad \text{and} \quad \|\mathbf{f} - \mathcal{P}_{k-1}^K(\mathbf{f})\|_{0,K} \leq C h_K^r |\mathbf{f}|_{r,K}.$$

Furthermore, similarly as for \mathbf{t} , we deduce from [12, Lemma 4.4] that when $\boldsymbol{\sigma}|_K \in \mathbb{H}^r(K)$ and $\boldsymbol{\sigma}^{\text{d}}|_K = \nabla \text{curl}(w)$ for some $w \in \mathbb{H}^{r+2}(K)$, with $1 \leq r \leq k+1$, there holds

$$\|\boldsymbol{\sigma} - \widehat{\Pi}^K(\boldsymbol{\sigma})\|_{0,K} \leq C h_K^r |\boldsymbol{\sigma}|_{r,K}.$$

However, certainly this is not the case in our present nonlinear problem since actually we find that

$$\boldsymbol{\sigma}^{\text{d}} = \mu(|\nabla \text{curl}(w)|) \nabla \text{curl}(w),$$

and therefore, unless $\mu(|\nabla \text{curl}(w)|)$ remains constant, we can not guarantee that the aforescribed choice of subspaces and projection gives optimal rates of convergence or just convergence. In fact, preliminary numerical experiments have reported that optimal rates of convergence are attained for \mathbf{t}_h and \mathbf{u}_h , but not for the remaining variables.

Consequently, being applicable only when the viscosity μ is constant, the mixed virtual element method proposed in this section constitutes a clear alternative to the approach from [12] for solving the Stokes problem. In particular, differently from [12], it provides a direct approximation of the velocity gradient. Further comparisons and corresponding numerical results will be reported somewhere else.

4.2 A second choice

In what follows we introduce a second choice of local subspaces and projection $\widehat{\Pi}^K$ yielding an optimally convergent mixed-VEM scheme (3.12) for our fully nonlinear problem. Indeed, given an integer $k \geq 0$, we now define for each $K \in \mathcal{T}_h$,

$$\begin{aligned} X^K &:= \left\{ \mathbf{s} \in \mathbb{P}_k(K) : \text{tr}(\mathbf{s}) = 0 \right\}, \\ H^K &:= \left\{ \boldsymbol{\tau} \in \mathbb{H}(\mathbf{div}; K) \cap \mathbb{H}(\mathbf{rot}; K) : \boldsymbol{\tau} \mathbf{n}|_e \in \mathbf{P}_k(e) \quad \forall \text{ edge } e \in \partial K, \right. \\ &\quad \left. \mathbf{div}(\boldsymbol{\tau}) \in \mathbf{P}_k(K), \quad \text{and} \quad \mathbf{rot}(\boldsymbol{\tau}) \in \mathbf{P}_{k-1}(K) \right\}, \\ Y^K &:= \mathbf{P}_k(K), \end{aligned} \tag{4.7}$$

where $\mathbf{P}_{-1}(K) := \{\mathbf{0}\}$. We recall here that the virtual subspace H^K was first introduced in [7] and recently utilized in [13] for a pseudostress-based formulation of the linear Brinkman problem. We then remark that, according to (4.7) and the results in [7], the assumptions **(A.1)**-**(A.5)** are clearly satisfied in this case as well. In particular, the spaces $\mathbb{H}(K)$ and $\mathbb{H}(\Omega)$ needed in **(A.5)** and **(A.6)** can be taken exactly as in (4.2).

Next, for each $K \in \mathcal{T}_h$ we let $\mathcal{P}_k^K : \mathbf{L}^2(K) \rightarrow \mathbf{P}_k(K)$ and $\mathcal{P}_k^K : \mathbb{L}^2(K) \rightarrow \mathbb{P}_k(K)$ be the orthogonal projectors with respect to the inner products of $\mathbf{L}^2(K)$ and $\mathbb{L}^2(K)$, respectively, and set $\widehat{H}^K := \mathbb{P}_k(K)$ and $\widehat{\Pi}^K := \mathcal{P}_k^K$. In this way, given $\boldsymbol{\zeta} \in \mathbb{L}^2(K)$, $\widehat{\Pi}^K(\boldsymbol{\zeta})$ is characterized by

$$\int_K \widehat{\Pi}^K(\boldsymbol{\zeta}) : \boldsymbol{\tau} = \int_K \boldsymbol{\zeta} : \boldsymbol{\tau} \quad \forall \boldsymbol{\tau} \in \mathbb{P}_k(K), \tag{4.8}$$

which obviously proves (3.9) in **(P.3)**, and from which it readily follows that (3.8) in **(P.2)** holds with $\widehat{c}_1 = 1$ and $\widehat{c}_2 = 0$. In turn, we notice that the property **(P.1)** was established in [7] (see also [13]).

Furthermore, taking $\boldsymbol{\zeta} = \mathbf{t}$ and $\boldsymbol{\tau} := \text{tr}(\mathcal{P}_k^K(\mathbf{t})) \mathbb{I}$ in (4.8), and bearing in mind that $\text{tr}(\mathbf{t}) = 0$, we deduce that $\text{tr}(\mathcal{P}_k^K(\mathbf{t})) = 0$, and hence $\mathcal{P}_X^h(\mathbf{t})|_K = \mathcal{P}_k^K(\mathbf{t})$ for all $K \in \mathcal{T}_h$. Thus, as a consequence again of Theorems 3.1, 3.2, 3.3, and 3.4, we obtain the following result.

Theorem 4.2. *Let X^K , H^K and Y^K be those described in (4.7), consider $\widehat{\Pi}^K = \mathcal{P}_k^K$ as defined in (4.8), and assume that the parameter κ lies in $\left(0, \frac{\alpha_0}{\gamma_0}\right)$, where γ_0 and α_0 are the positive constants from (2.2) and (2.3), respectively. Then the Galerkin scheme (3.12) has a unique solution $((\mathbf{t}_h, \boldsymbol{\sigma}_h), \mathbf{u}_h) \in (X_h \times H_h) \times Y_h$ and there exist positive constants $C_1, C_2 > 0$, independent of h , such that*

$$\|\mathbf{t}_h\|_{0,\Omega} + \|\boldsymbol{\sigma}_h\|_{\mathbf{div};\Omega} + \|\mathbf{u}_h\|_{0,\Omega} \leq C_1 \left\{ \|\mathbf{f}\|_{0,\Omega} + \|\mathbf{g}\|_{1/2,\Gamma} \right\},$$

$$\begin{aligned} & \|\mathbf{t} - \mathbf{t}_h\|_{0,\Omega} + \|\boldsymbol{\sigma} - \boldsymbol{\sigma}_h\|_{0,\Omega} + \|p - p_h\|_{0,\Omega} + \|\boldsymbol{\sigma} - \widehat{\boldsymbol{\sigma}}_h\|_{0,\Omega} + \|p - \widehat{p}_h\|_{0,\Omega} \\ & \leq C_2 \sum_{K \in \mathcal{T}_h} \left\{ \|\mathbf{t} - \mathcal{P}_k^K(\mathbf{t})\|_{0,K} + \|\boldsymbol{\sigma} - \Pi^K(\boldsymbol{\sigma})\|_{0,K} + \|\boldsymbol{\sigma} - \mathcal{P}_k^K(\boldsymbol{\sigma})\|_{0,K} + h_K \|\mathbf{f} - \mathcal{P}_k^K(\mathbf{f})\|_{0,K} \right\}, \end{aligned}$$

and

$$\begin{aligned} \|\mathbf{u} - \mathbf{u}_h\|_{0,\Omega} & \leq C_2 \sum_{K \in \mathcal{T}_h} \left\{ \|\mathbf{t} - \mathcal{P}_k^K(\mathbf{t})\|_{0,K} + \|\boldsymbol{\sigma} - \Pi^K(\boldsymbol{\sigma})\|_{0,K} \right. \\ & \quad \left. + \|\boldsymbol{\sigma} - \mathcal{P}_k^K(\boldsymbol{\sigma})\|_{0,K} + \|\mathbf{u} - \mathcal{P}_k^K(\mathbf{u})\|_{0,K} + h_K \|\mathbf{f} - \mathcal{P}_k^K(\mathbf{f})\|_{0,K} \right\}, \end{aligned}$$

where $p_h \in L^2(\Omega)$ is the postprocessed virtual pressure defined in (3.13), and $\widehat{\boldsymbol{\sigma}}_h$ and \widehat{p}_h are the fully computable discrete approximations introduced in (3.42).

We now recall from [12, Lemma 3.4] and [7, eqs. (22) and (28)] the approximation properties of the operators \mathcal{P}_k^K , \mathcal{P}_k^K and Π^K , respectively. In fact, given $K \in \mathcal{T}_h$, $0 \leq \ell \leq k+1$, and $1 \leq m \leq k+1$, there hold

$$\|\mathbf{v} - \mathcal{P}_k^K(\mathbf{v})\|_{0,K} \leq C h_K^\ell |\mathbf{v}|_{\ell,K} \quad \forall \mathbf{v} \in \mathbf{H}^\ell(K), \quad (4.9)$$

$$\|\zeta - \mathcal{P}_k^K(\zeta)\|_{0,K} \leq C h_K^\ell |\zeta|_{\ell,K} \quad \forall \zeta \in \mathbb{H}^\ell(K), \quad (4.10)$$

and

$$\|\zeta - \Pi^K(\zeta)\|_{0,K} \leq C h_K^m |\zeta|_{m,K} \quad \forall \zeta \in \mathbb{H}^m(K). \quad (4.11)$$

Then, as a consequence of the foregoing estimates and Theorem 4.2, we are able to provide next the rates of convergence of our mixed virtual element scheme (3.12).

Theorem 4.3. *In addition to the notations and hypotheses from Theorem 4.2, assume that for some $r \in [1, k+1]$ there hold $\mathbf{t}|_K, \boldsymbol{\sigma}|_K \in \mathbb{H}^r(K)$, $\mathbf{u}|_K \in \mathbf{H}^r(K)$ and $\mathbf{f}|_K \in \mathbf{H}^{r-1}(K)$ for each $K \in \mathcal{T}_h$. Then, there exists $C > 0$, independent of h , such that*

$$\begin{aligned} & \|\mathbf{t} - \mathbf{t}_h\|_{0,\Omega} + \|\boldsymbol{\sigma} - \boldsymbol{\sigma}_h\|_{0,\Omega} + \|p - p_h\|_{0,\Omega} + \|\boldsymbol{\sigma} - \widehat{\boldsymbol{\sigma}}_h\|_{0,\Omega} + \|p - \widehat{p}_h\|_{0,\Omega} \\ & \leq C h^r \sum_{K \in \mathcal{T}_h} \left\{ |\mathbf{t}|_{r,K} + |\boldsymbol{\sigma}|_{r,K} + |\mathbf{f}|_{r-1,K} \right\}, \end{aligned}$$

and

$$\|\mathbf{u} - \mathbf{u}_h\|_{0,\Omega} \leq C h^r \sum_{K \in \mathcal{T}_h} \left\{ |\mathbf{t}|_{r,K} + |\boldsymbol{\sigma}|_{r,K} + |\mathbf{u}|_{r,K} + |\mathbf{f}|_{r-1,K} \right\}.$$

4.3 A convergent approximation of $\boldsymbol{\sigma}$ in the broken $\mathbb{H}(\mathbf{div}; \Omega)$ -norm

In this section we proceed as in [13, Section 5.3] and construct a second approximation, denoted $\boldsymbol{\sigma}_h^*$, for the pseudostress variable $\boldsymbol{\sigma}$, which has an optimal rate of convergence in the broken $\mathbb{H}(\mathbf{div})$ -norm. To this end, for each $K \in \mathcal{T}_h$ we let $(\cdot, \cdot)_{\mathbf{div};K}$ be the usual $\mathbb{H}(\mathbf{div}; K)$ -inner product with induced norm $\|\cdot\|_{\mathbf{div};K}$, and set $\boldsymbol{\sigma}_h^*|_K := \boldsymbol{\sigma}_{h,K}^*$, where $\boldsymbol{\sigma}_{h,K}^* \in \mathbb{P}_{k+1}(K)$ is the unique solution of the local problem

$$(\boldsymbol{\sigma}_{h,K}^*, \boldsymbol{\tau}_h)_{\mathbf{div};K} = \int_K \widehat{\boldsymbol{\sigma}}_h : \boldsymbol{\tau}_h + \int_K \mathbf{div}(\boldsymbol{\sigma}_h) \cdot \mathbf{div}(\boldsymbol{\tau}_h) \quad \forall \boldsymbol{\tau}_h \in \mathbb{P}_{k+1}(K). \quad (4.12)$$

We highlight that $\boldsymbol{\sigma}_{h,K}^*$ can be explicitly calculated for each $K \in \mathcal{T}_h$, independently. Then, the rate of convergence for the broken $\mathbb{H}(\mathbf{div}; \Omega)$ -norm of $\boldsymbol{\sigma} - \boldsymbol{\sigma}_h^*$ is established as follows.

Theorem 4.4. *In addition to the hypotheses of Theorem 4.3, assume that for some $r \in [1, k+1]$ there holds $\mathbf{f}|_K = -\mathbf{div}(\boldsymbol{\sigma})|_K \in \mathbf{H}^r(K)$ for each $K \in \mathcal{T}_h$. Then, there exists a positive constant C , independent of h , such that*

$$\left\{ \sum_{K \in \mathcal{T}_h} \|\boldsymbol{\sigma} - \boldsymbol{\sigma}_h^*\|_{\mathbf{div};K}^2 \right\}^{1/2} \leq C h^r \sum_{K \in \mathcal{T}_h} \left\{ |\mathbf{t}|_{r,K} + |\boldsymbol{\sigma}|_{r,K} + |\mathbf{f}|_{r,K} \right\}.$$

Proof. From [13, Lemma 5.3] and the first part in the proof of [13, Theorem 5.5], we find that there exists $C > 0$, independent of h , such that for each $K \in \mathcal{T}_h$ there holds

$$\begin{aligned} \|\boldsymbol{\sigma} - \boldsymbol{\sigma}_{h,K}^*\|_{\mathbf{div};K} & \leq C \left\{ \|\boldsymbol{\sigma} - \widehat{\boldsymbol{\sigma}}_h\|_{0,K} + \|\mathbf{div}(\boldsymbol{\sigma} - \boldsymbol{\sigma}_h)\|_{0,K} \right. \\ & \quad \left. + \|\boldsymbol{\sigma} - \mathcal{P}_{k+1}^K(\boldsymbol{\sigma})\|_{0,K} + |\boldsymbol{\sigma} - \mathcal{P}_{k+1}^K(\boldsymbol{\sigma})|_{1,K} \right\}, \end{aligned}$$

where $\mathcal{P}_{k+1}^K : \mathbb{L}^2(K) \rightarrow \mathbb{P}_{k+1}(K)$ is the $\mathbb{L}^2(K)$ -orthogonal projector. Thus, employing from (3.24) that $\|\mathbf{div}(\boldsymbol{\sigma} - \boldsymbol{\sigma}_h)\|_{0,K} = \|\mathbf{f} - \mathcal{P}_k^K(\mathbf{f})\|_{0,K}$, the foregoing estimate becomes

$$\begin{aligned} \|\boldsymbol{\sigma} - \boldsymbol{\sigma}_{h,K}^*\|_{\mathbf{div};K} &\leq C \left\{ \|\boldsymbol{\sigma} - \widehat{\boldsymbol{\sigma}}_h\|_{0,K} + \|\mathbf{f} - \mathcal{P}_k^K(\mathbf{f})\|_{0,K} \right. \\ &\quad \left. + \|\boldsymbol{\sigma} - \mathcal{P}_{k+1}^K(\boldsymbol{\sigma})\|_{0,K} + |\boldsymbol{\sigma} - \mathcal{P}_{k+1}^K(\boldsymbol{\sigma})|_{1,K} \right\}. \end{aligned}$$

Finally, the result follows after applying the estimate for $\|\boldsymbol{\sigma} - \widehat{\boldsymbol{\sigma}}_h\|_{0,K}$ (cf. Theorem 4.3), and the approximation properties of \mathcal{P}_k^K (cf. (4.9)) and \mathcal{P}_{k+1}^K (cf. [12, Lemma 3.4]). \square

5 Numerical results

In this section we present three numerical experiments illustrating the performance of the augmented mixed virtual element scheme (3.12) introduced and analyzed in Sections 3 and 4. More precisely, in all the computations we consider the specific virtual element subspaces X_h , H_h and Y_h (cf. (3.1)-(3.2)-(3.3)) and associated discrete nonlinear operator \mathcal{A}_h (cf. (3.11)) determined by the definitions of the local subspaces X^K , H^K , and Y^K , and projectors $\widehat{\Pi}^K$, respectively, described in our second choice (cf. Section 4.2) with $k \in \{0, 1, 2\}$. In addition, as it is mentioned in [13], the zero mean condition for tensors in the space H_h is imposed via a real Lagrange multiplier, which means that, instead of (3.12), we solve the modified discrete scheme given by: Find $((\mathbf{t}_h, \boldsymbol{\sigma}_h), (\mathbf{u}_h, \xi_h)) \in (X_h \times \widetilde{H}_h) \times (Y_h \times \mathbb{R})$ such that

$$\begin{aligned} [\mathcal{A}_h(\mathbf{t}_h, \boldsymbol{\sigma}_h), (\mathbf{s}_h, \boldsymbol{\tau}_h)] + [\mathcal{B}(\mathbf{s}_h, \boldsymbol{\tau}_h), \mathbf{u}_h] + \xi_h \int_{\Omega} \text{tr}(\boldsymbol{\tau}_h) &= [\mathcal{F}, (\mathbf{s}_h, \boldsymbol{\tau}_h)], \\ [\mathcal{B}(\mathbf{t}_h, \boldsymbol{\sigma}_h), \mathbf{v}_h] + \eta_h \int_{\Omega} \text{tr}(\boldsymbol{\sigma}_h) &= [\mathcal{G}, \mathbf{v}_h], \end{aligned} \tag{5.1}$$

for all $((\mathbf{s}_h, \boldsymbol{\tau}_h), (\mathbf{v}_h, \eta_h)) \in (X_h \times \widetilde{H}_h) \times (Y_h \times \mathbb{R})$, where

$$\widetilde{H}_h := \left\{ \boldsymbol{\tau} \in \mathbb{H}(\mathbf{div}; \Omega) : \boldsymbol{\tau}|_K \in H^K \quad \forall K \in \mathcal{T}_h \right\},$$

and ξ_h is an artificial unknown introduced just to keep the symmetry of (3.12). Concerning the decompositions of Ω employed in our computations, we consider quasi-uniform triangles, distorted squares and distorted hexagons.

We begin by introducing additional notations. In what follows, N stands for the total number of degrees of freedom (unknowns) of (5.1), that is,

$$N := 2(k+1) \times \{\text{number of edges } e \in \mathcal{T}_h\} + \frac{(k+2)(9k+5)}{2} \times \{\text{number of elements } K \in \mathcal{T}_h\} + 1.$$

Also, the individual errors are defined by

$$\begin{aligned} \mathbf{e}(\mathbf{t}) &:= \|\mathbf{t} - \mathbf{t}_h\|_{0,\Omega}, \quad \mathbf{e}(\boldsymbol{\sigma}) := \|\boldsymbol{\sigma} - \widehat{\boldsymbol{\sigma}}_h\|_{0,\Omega}, \quad \mathbf{e}(\mathbf{u}) := \|\mathbf{u} - \mathbf{u}_h\|_{0,\Omega}, \\ \mathbf{e}(p) &:= \|p - \widehat{p}_h\|_{0,\Omega} \quad \text{and} \quad \mathbf{e}(\boldsymbol{\sigma}^*) := \left\{ \sum_{K \in \mathcal{T}_h} \|\boldsymbol{\sigma} - \boldsymbol{\sigma}_h^*\|_{\mathbf{div};K}^2 \right\}^{1/2}, \end{aligned}$$

where $(\widehat{\boldsymbol{\sigma}}_h, \widehat{p}_h)$, and $\boldsymbol{\sigma}_h^*$ are computed according to (3.42) and (4.12), respectively. In turn, the associated experimental rates of convergence are given by

$$\mathbf{r}(\cdot) := \frac{\log(\mathbf{e}(\cdot)/\mathbf{e}'(\cdot))}{\log(h/h')},$$

where \mathbf{e} and \mathbf{e}' denote the corresponding errors for two consecutive meshes with sizes h and h' , respectively.

The corresponding nonlinear algebraic system arising from (5.1) is solved by the Newton method with a tolerance of 10^{-6} and taking as initial iteration the solution of the associated linear Stokes problem (four iterations were required to achieve the given tolerance in each example). The numerical results presented below were obtained using a MATLAB code, where the corresponding linear systems were solved using its instruction “\” as main solver.

In Example 1 we consider the linear Stokes problem associated with the data: $\Omega := (0, 1)^2$ and $\mu = \frac{1}{2}$, along with \mathbf{f} and \mathbf{g} chosen so that the exact solution is given by

$$\mathbf{u}(\mathbf{x}) = \begin{pmatrix} x_1^2 \exp(-x_1)(1+x_2)(2 \sin(1+x_2) + (1+x_2) \cos(1+x_2)) \\ x_1(x_1-2) \exp(-x_1)(1+x_2)^2 \sin(1+x_2) \end{pmatrix}$$

and

$$p(\mathbf{x}) = \sin(2\pi x_1) \sin(2\pi x_2),$$

for all $\mathbf{x} := (x_1, x_2)^\top \in \Omega$.

In Example 2 we deal with the nonlinear version of Example 1. More precisely, we consider instead of $\mu = \frac{1}{2}$ the kinematic viscosity function $\mu : \mathbb{R}^+ \rightarrow \mathbb{R}^+$ given by the Carreau law:

$$\mu(t) := \kappa_0 + \kappa_1(1+t^2)^{(\beta-2)/2} \quad \forall t \in \mathbb{R}^+,$$

with $\kappa_0 = \kappa_1 = \frac{1}{2}$ and $\beta = \frac{3}{2}$. It is easy to check in this case that the assumptions (2.2) and (2.3) are satisfied with

$$\gamma_0 = \kappa_0 + \kappa_1 \left\{ \frac{|\beta-2|}{2} + 1 \right\} \quad \text{and} \quad \alpha_0 = \kappa_0.$$

On the other hand, we take the stabilization parameter $\kappa := \frac{\alpha_0}{2\gamma_0^2}$ which obviously satisfies the assumption required in Lemma 3.3. Then, we let again $\Omega := (0, 1)^2$, and choose the data \mathbf{f} and \mathbf{g} so that the exact solution is the same from Example 1. The set of decompositions utilized is also as in Example 1.

Finally, in Example 3 we follow [24] and consider the same nonlinearity μ from Example 2, together with the L -shaped domain $\Omega := (-1, 1)^2 \setminus [0, 1]^2$, and choose the data \mathbf{f} and \mathbf{g} so that the exact solution is given by

$$\mathbf{u}(\mathbf{x}) = \begin{pmatrix} r^{2/3} \sin(\theta) \\ -r^{2/3} \cos(\theta) \end{pmatrix} \quad \text{and} \quad p(\mathbf{x}) = \cos(x_1) \cos(x_2) - \sin^2(1),$$

for all $\mathbf{x} := (x_1, x_2)^\top \in \Omega$, where $r := |\mathbf{x}| = \sqrt{x_1^2 + x_2^2}$ and $\theta := \arctan\left(\frac{x_2}{x_1}\right)$. Note in this example that $\nabla \mathbf{u}$ is singular at the origin, and hence lower rates of convergence are expected in our computations. More precisely, there holds $\mathbf{u} \in \mathbf{H}^{5/3-\epsilon}(\Omega)$, which implies that $\mathbf{t}, \boldsymbol{\sigma} \in \mathbb{H}^{2/3-\epsilon}(\Omega)$ and $\mathbf{div}(\boldsymbol{\sigma}) \in \mathbf{H}^{-1/3-\epsilon}(\Omega)$ for each $\epsilon > 0$.

In Tables 5.1 up to 5.6, we summarize the convergence history of the augmented mixed virtual element scheme (5.1) as applied to Example 1 and 2. We notice there that the rate of convergence $O(h^{k+1})$ predicted by Theorems 4.3 and 4.4 (when $r = k + 1$) is attained by all the unknowns for these smooth examples, for triangular as well as for quadrilateral and hexagonal meshes. In particular, these results confirm that our postprocessed stress $\boldsymbol{\sigma}_h^*$ improves in one power the non-satisfactory order provided by the first approximation $\widehat{\boldsymbol{\sigma}}_h$ with respect to the broken $\mathbb{H}(\mathbf{div})$ -norm (results that are not reported here). Next, in Tables 5.7, 5.8 and 5.9, we provide the convergence history of Example 3. As predicted in advance, and due to the singularity at the origin of \mathbf{u} in this case, we observe that

the orders $O(h^{2/3})$ and $O(h^{5/3})$ are attained by $(\boldsymbol{\sigma}, p)$ and \mathbf{u} , respectively. Moreover, $\boldsymbol{\sigma}_h^*$ attained $O(h^{-1/3})$ (cf. Theorem 4.4) because $\mathbf{f} = -\mathbf{div}(\boldsymbol{\sigma}) \in \mathbf{H}^{-1/3-\epsilon}(\Omega)$ for each $\epsilon > 0$. A very common way to overcome this drawback is the use of adaptive algorithms based on suitable *a posteriori* error estimators. This issue will be addressed in a forthcoming work.

Finally, in order to graphically illustrate the accurateness of our discrete scheme, in Figure 5.1 we display some components of the approximate solutions for Example 2. They all correspond to those obtained with the first mesh of each kind (triangles, quadrilaterals and hexagons, respectively) and for the polynomial degree $k = 2$.

k	h	N	$\mathbf{e}(\mathbf{t})$	$\mathbf{r}(\mathbf{t})$	$\mathbf{e}(\boldsymbol{\sigma})$	$\mathbf{r}(\boldsymbol{\sigma})$	$\mathbf{e}(\mathbf{u})$	$\mathbf{r}(\mathbf{u})$	$\mathbf{e}(p)$	$\mathbf{r}(p)$	$\mathbf{e}(\boldsymbol{\sigma}^*)$	$\mathbf{r}(\boldsymbol{\sigma}^*)$
0	0.0643	7833	1.35e-1	---	1.57e-1	---	2.53e-2	---	5.72e-2	---	5.11e-1	---
	0.0488	13573	1.03e-1	0.98	1.18e-1	1.02	1.92e-2	1.00	4.15e-2	1.15	3.88e-1	1.00
	0.0248	52213	5.26e-2	0.99	5.96e-2	1.02	9.75e-3	1.00	1.97e-2	1.10	1.97e-1	1.00
	0.0166	115941	3.54e-2	1.00	3.98e-2	1.01	6.53e-3	1.00	1.30e-2	1.05	1.32e-1	1.00
	0.0129	194041	2.73e-2	1.00	3.07e-2	1.01	5.05e-3	1.00	9.94e-3	1.03	1.02e-1	1.00
1	0.0643	26313	2.61e-3	---	7.32e-3	---	5.74e-4	---	4.84e-3	---	2.45e-2	---
	0.0488	45647	1.42e-3	2.20	3.96e-3	2.22	3.31e-4	2.00	2.61e-3	2.23	1.41e-2	2.02
	0.0248	175903	3.14e-4	2.23	8.38e-4	2.30	8.56e-5	2.00	5.49e-4	2.31	3.59e-3	2.02
	0.0166	390831	1.34e-4	2.14	3.42e-4	2.24	3.85e-5	2.00	2.23e-4	2.26	1.61e-3	2.01
	0.0129	654281	7.89e-5	2.05	1.96e-4	2.16	2.30e-5	2.00	1.27e-4	2.18	9.59e-4	2.01
2	0.0643	53505	6.37e-5	---	1.96e-4	---	7.20e-6	---	1.31e-4	---	9.58e-4	---
	0.0488	92859	2.77e-5	3.02	8.52e-5	3.02	3.14e-6	3.00	5.70e-5	3.02	4.19e-4	3.00
	0.0248	358075	3.62e-6	3.01	1.11e-5	3.01	4.14e-7	3.00	7.45e-6	3.01	5.52e-5	3.00
	0.0166	795771	1.09e-6	3.00	3.35e-6	3.01	1.25e-7	3.00	2.24e-6	3.01	1.66e-5	3.00
	0.0129	1332321	5.04e-7	3.00	1.55e-6	3.00	5.76e-8	3.00	1.03e-6	3.00	7.68e-6	3.00

Table 5.1: Example 1, history of convergence using triangles.

k	h	N	$\mathbf{e}(\mathbf{t})$	$\mathbf{r}(\mathbf{t})$	$\mathbf{e}(\boldsymbol{\sigma})$	$\mathbf{r}(\boldsymbol{\sigma})$	$\mathbf{e}(\mathbf{u})$	$\mathbf{r}(\mathbf{u})$	$\mathbf{e}(p)$	$\mathbf{r}(p)$	$\mathbf{e}(\boldsymbol{\sigma}^*)$	$\mathbf{r}(\boldsymbol{\sigma}^*)$
0	0.0538	8221	7.99e-2	---	1.03e-1	---	2.37e-2	---	4.58e-2	---	4.42e-1	---
	0.0404	14561	6.01e-2	0.99	7.75e-2	0.98	1.78e-2	1.00	3.47e-2	0.97	3.32e-1	1.00
	0.0215	50926	3.20e-2	1.00	4.07e-2	1.03	9.49e-3	1.00	1.77e-2	1.07	1.77e-1	1.00
	0.0147	109341	2.18e-2	1.00	2.76e-2	1.01	6.47e-3	1.00	1.20e-2	1.02	1.21e-1	1.00
	0.0111	189806	1.65e-2	1.00	2.10e-2	1.00	4.91e-3	1.00	9.11e-3	1.00	9.15e-2	1.00
1	0.0538	26341	7.19e-3	---	6.58e-2	---	3.94e-4	---	4.62e-2	---	6.44e-2	---
	0.0404	46721	3.75e-3	2.27	3.22e-2	2.49	2.20e-4	2.02	2.26e-2	2.49	3.18e-2	2.46
	0.0215	163726	8.20e-4	2.42	6.52e-3	2.54	6.24e-5	2.01	4.57e-3	2.54	6.74e-3	2.47
	0.0147	351781	3.29e-4	2.38	2.49e-3	2.52	2.90e-5	2.00	1.74e-3	2.52	2.71e-3	2.38
	0.0111	610886	1.71e-4	2.37	1.31e-3	2.33	1.67e-5	2.00	9.17e-4	2.33	1.47e-3	2.22
2	0.0538	52561	2.21e-4	---	9.78e-3	---	4.54e-6	---	6.91e-3	---	8.80e-3	---
	0.0404	93281	9.40e-5	2.98	4.01e-3	3.10	1.89e-6	3.05	2.83e-3	3.10	3.61e-3	3.10
	0.0215	327151	1.26e-5	3.20	4.02e-4	3.66	2.82e-7	3.03	2.84e-4	3.66	3.63e-4	3.66
	0.0147	703121	4.02e-6	2.98	1.18e-4	3.19	8.91e-8	3.01	8.37e-5	3.19	1.07e-4	3.18
	0.0111	1221191	1.72e-6	3.07	4.57e-5	3.45	3.89e-8	3.00	3.23e-5	3.45	4.13e-5	3.45

Table 5.2: Example 1, history of convergence using quadrilaterals.

k	h	N	$\mathbf{e}(\mathbf{t})$	$\mathbf{r}(\mathbf{t})$	$\mathbf{e}(\boldsymbol{\sigma})$	$\mathbf{r}(\boldsymbol{\sigma})$	$\mathbf{e}(\mathbf{u})$	$\mathbf{r}(\mathbf{u})$	$\mathbf{e}(p)$	$\mathbf{r}(p)$	$\mathbf{e}(\boldsymbol{\sigma}^*)$	$\mathbf{r}(\boldsymbol{\sigma}^*)$
0	0.0488	11201	9.74e-2	--	7.92e-0	--	2.16e-2	--	5.60e-0	--	7.93e-0	--
	0.0377	18675	8.91e-2	0.34	6.55e-0	0.74	1.70e-2	0.90	4.63e-0	0.74	6.55e-0	0.74
	0.0277	33795	5.80e-2	1.41	5.08e-0	0.83	1.24e-2	1.04	3.59e-0	0.83	5.08e-0	0.83
	0.0197	66828	4.29e-2	0.88	3.57e-0	1.02	8.78e-3	1.01	2.53e-0	1.02	3.58e-0	1.02
	0.0146	121943	3.08e-2	1.10	2.67e-0	0.96	6.50e-3	1.00	1.89e-0	0.96	2.68e-0	0.96
1	0.0488	33599	3.06e-3	--	2.74e-1	--	3.25e-4	--	1.93e-1	--	2.59e-1	--
	0.0377	56093	2.00e-3	1.63	1.56e-1	2.16	1.96e-4	1.95	1.10e-1	2.16	1.47e-1	2.19
	0.0277	101381	1.05e-3	2.13	8.61e-2	1.95	1.06e-4	2.00	6.09e-2	1.95	8.08e-2	1.96
	0.0197	200480	5.22e-4	2.03	4.25e-2	2.05	5.31e-5	2.01	3.01e-2	2.05	3.99e-2	2.05
	0.0146	366007	2.89e-4	1.97	2.27e-2	2.09	2.93e-5	1.98	1.60e-2	2.09	2.12e-2	2.10
2	0.0488	65159	5.18e-5	--	8.60e-3	--	3.13e-6	--	6.08e-3	--	7.45e-3	--
	0.0377	108847	2.33e-5	3.08	3.86e-3	3.09	1.46e-6	2.93	2.73e-3	3.09	3.34e-3	3.09
	0.0277	196615	8.77e-6	3.20	1.36e-3	3.41	5.83e-7	3.01	9.62e-4	3.41	1.17e-3	3.43
	0.0197	388807	3.21e-6	2.92	4.82e-4	3.01	2.07e-7	3.01	3.41e-4	3.01	4.17e-4	3.01
	0.0146	709989	1.27e-6	3.08	1.79e-4	3.30	8.46e-8	2.98	1.26e-4	3.30	1.54e-4	3.30

Table 5.3: Example 1, history of convergence using hexagons.

k	h	N	$\mathbf{e}(\mathbf{t})$	$\mathbf{r}(\mathbf{t})$	$\mathbf{e}(\boldsymbol{\sigma})$	$\mathbf{r}(\boldsymbol{\sigma})$	$\mathbf{e}(\mathbf{u})$	$\mathbf{r}(\mathbf{u})$	$\mathbf{e}(p)$	$\mathbf{r}(p)$	$\mathbf{e}(\boldsymbol{\sigma}^*)$	$\mathbf{r}(\boldsymbol{\sigma}^*)$
0	0.0643	7833	1.27e-1	--	2.03e-1	--	2.53e-2	--	6.11e-2	--	5.66e-1	--
	0.0488	13573	9.66e-2	0.98	1.53e-1	1.02	1.92e-2	1.00	4.38e-2	1.20	4.29e-1	1.00
	0.0248	52213	4.94e-2	0.99	7.72e-2	1.01	9.74e-3	1.00	2.04e-2	1.13	2.18e-1	1.00
	0.0166	115941	3.32e-2	1.00	5.16e-2	1.01	6.53e-3	1.00	1.33e-2	1.07	1.46e-1	1.00
	0.0129	194041	2.56e-2	1.00	3.99e-2	1.00	5.05e-3	1.00	1.02e-2	1.04	1.13e-1	1.00
1	0.0643	26313	2.48e-3	--	9.18e-3	--	5.74e-4	--	6.00e-3	--	2.56e-2	--
	0.0488	45647	1.34e-3	2.23	4.78e-3	2.36	3.31e-4	2.00	3.12e-3	2.37	1.46e-2	2.04
	0.0248	175903	3.00e-4	2.21	9.35e-4	2.42	8.56e-5	2.00	5.96e-4	2.45	3.68e-3	2.03
	0.0166	390831	1.30e-4	2.10	3.73e-4	2.30	3.85e-5	2.00	2.33e-4	2.35	1.65e-3	2.02
	0.0129	654281	7.71e-5	2.03	2.12e-4	2.20	2.30e-5	2.00	1.31e-4	2.24	9.80e-4	2.01
2	0.0643	53505	4.26e-5	--	1.98e-4	--	7.20e-6	--	1.32e-4	--	9.77e-4	--
	0.0488	92859	1.85e-5	3.03	8.59e-5	3.03	3.14e-6	3.00	5.73e-5	3.03	4.27e-4	3.00
	0.0248	358075	2.41e-6	3.01	1.12e-5	3.02	4.14e-7	3.00	7.45e-6	3.02	5.63e-5	3.00
	0.0166	795771	7.26e-7	3.00	3.36e-6	3.01	1.25e-7	3.00	2.24e-6	3.01	1.70e-5	3.00
	0.0129	1332321	3.33e-7	3.02	1.53e-6	3.05	5.76e-8	3.00	1.02e-6	3.03	7.83e-6	3.00

Table 5.4: Example 2, history of convergence using triangles.

k	h	N	$\mathbf{e}(\mathbf{t})$	$\mathbf{r}(\mathbf{t})$	$\mathbf{e}(\boldsymbol{\sigma})$	$\mathbf{r}(\boldsymbol{\sigma})$	$\mathbf{e}(\mathbf{u})$	$\mathbf{r}(\mathbf{u})$	$\mathbf{e}(p)$	$\mathbf{r}(p)$	$\mathbf{e}(\boldsymbol{\sigma}^*)$	$\mathbf{r}(\boldsymbol{\sigma}^*)$
0	0.0538	8221	7.99e-2	--	1.35e-1	--	2.37e-2	--	4.78e-2	--	4.78e-1	--
	0.0404	14561	6.00e-2	0.99	1.01e-1	0.99	1.78e-2	1.00	3.63e-2	0.96	3.59e-1	1.00
	0.0215	50926	3.20e-2	1.00	5.32e-2	1.03	9.49e-3	1.00	1.81e-2	1.10	1.91e-1	1.00
	0.0147	109341	2.18e-2	1.00	3.61e-2	1.01	6.47e-3	1.00	1.22e-2	1.04	1.31e-1	1.00
	0.0111	189806	1.65e-2	1.00	2.74e-2	1.00	4.91e-3	1.00	9.24e-3	1.00	9.90e-2	1.00
1	0.0538	26341	5.54e-3	--	7.14e-2	--	3.91e-4	--	5.02e-2	--	6.95e-2	--
	0.0404	46721	2.95e-3	2.20	3.51e-2	2.47	2.20e-4	2.01	2.46e-2	2.48	3.43e-2	2.45
	0.0215	163726	6.58e-4	2.38	7.10e-3	2.54	6.24e-5	2.00	4.98e-3	2.54	7.22e-3	2.48
	0.0147	351781	2.68e-4	2.35	2.71e-3	2.51	2.90e-5	2.00	1.90e-3	2.51	2.90e-3	2.39
	0.0111	610886	1.41e-4	2.33	1.44e-3	2.31	1.67e-5	2.00	1.01e-3	2.31	1.57e-3	2.22
2	0.0538	52561	1.90e-4	--	1.04e-2	--	4.48e-6	--	7.35e-3	--	9.33e-3	--
	0.0404	93281	8.15e-5	2.96	4.32e-3	3.06	1.88e-6	3.03	3.05e-3	3.06	3.88e-3	3.06
	0.0215	327151	1.13e-5	3.14	4.52e-4	3.59	2.82e-7	3.02	3.19e-4	3.59	4.06e-4	3.59
	0.0147	703121	3.63e-6	2.97	1.35e-4	3.15	8.90e-8	3.01	9.56e-5	3.15	1.22e-4	3.14
	0.0111	1221191	1.58e-6	3.01	5.75e-5	3.10	3.87e-8	3.02	4.10e-5	3.06	5.23e-5	3.06

Table 5.5: Example 2, history of convergence using quadrilaterals.

k	h	N	$e(t)$	$r(t)$	$e(\sigma)$	$r(\sigma)$	$e(u)$	$r(u)$	$e(p)$	$r(p)$	$e(\sigma^*)$	$r(\sigma^*)$
0	0.0488	11201	9.29e-2	--	7.99e-0	--	2.15e-2	--	5.65e-0	--	8.00e-0	--
	0.0377	18675	8.22e-2	0.47	6.61e-0	0.73	1.69e-2	0.93	4.67e-0	0.73	6.61e-0	0.74
	0.0277	33795	5.47e-2	1.34	5.12e-0	0.83	1.23e-2	1.02	3.62e-0	0.83	5.13e-0	0.83
	0.0197	66828	4.02e-2	0.89	3.61e-0	1.02	8.75e-3	1.00	2.55e-0	1.02	3.61e-0	1.02
	0.0146	121943	2.90e-2	1.09	2.70e-0	0.97	6.49e-3	1.00	1.91e-0	0.96	2.70e-0	0.97
1	0.0488	33599	2.76e-3	--	2.75e-1	--	3.22e-4	--	1.94e-1	--	2.60e-1	--
	0.0377	56093	1.82e-3	1.61	1.57e-1	2.15	1.95e-4	1.93	1.11e-1	2.15	1.48e-1	2.18
	0.0277	101381	9.46e-4	2.14	8.65e-2	1.95	1.06e-4	2.00	6.12e-2	1.95	8.12e-2	1.96
	0.0197	200480	4.77e-4	1.99	4.27e-2	2.05	5.31e-5	2.01	3.02e-2	2.05	4.02e-2	2.05
	0.0146	366007	2.64e-4	1.97	2.28e-2	2.09	2.93e-5	1.98	1.61e-2	2.09	2.13e-2	2.10
2	0.0488	65159	4.57e-5	--	8.77e-3	--	3.11e-6	--	6.20e-3	--	7.61e-3	--
	0.0377	108847	2.09e-5	3.02	3.92e-3	3.10	1.46e-6	2.92	2.77e-3	3.10	3.40e-3	3.11
	0.0277	196615	7.80e-6	3.22	1.39e-3	3.40	5.82e-7	3.00	9.80e-4	3.40	1.20e-3	3.42
	0.0197	388807	2.85e-6	2.92	4.91e-4	3.01	2.07e-7	3.01	3.47e-4	3.01	4.25e-4	3.01
	0.0146	709989	1.15e-6	3.01	2.04e-4	2.92	8.37e-8	3.01	1.40e-4	3.02	1.69e-4	3.08

Table 5.6: Example 2, history of convergence using hexagons.

k	h	N	$e(t)$	$r(t)$	$e(\sigma)$	$r(\sigma)$	$e(u)$	$r(u)$	$e(p)$	$r(p)$	$e(\sigma^*)$	$r(\sigma^*)$
0	0.1179	7009	1.20e-1	--	2.19e-1	--	4.69e-2	--	9.35e-2	--	4.62e-0	--
	0.0786	15697	9.26e-2	0.63	1.60e-1	0.78	3.13e-2	1.00	6.30e-2	0.97	5.19e-0	-0.29
	0.0429	52537	6.27e-2	0.64	1.01e-1	0.75	1.71e-2	1.00	3.60e-2	0.92	6.19e-0	-0.29
	0.0289	115641	4.85e-2	0.65	7.58e-2	0.73	1.15e-2	1.00	2.56e-2	0.87	6.96e-0	-0.29
	0.0218	203321	4.03e-2	0.65	6.18e-2	0.73	8.67e-3	1.00	2.02e-2	0.83	7.56e-0	-0.30
1	0.1179	23521	7.80e-2	--	1.80e-1	--	1.73e-3	--	9.88e-2	--	4.07e-0	--
	0.0786	52777	5.97e-2	0.66	1.33e-1	0.74	9.44e-4	1.49	7.24e-2	0.77	4.58e-0	-0.29
	0.0429	176947	4.00e-2	0.66	8.58e-2	0.73	3.91e-4	1.46	4.60e-2	0.75	5.48e-0	-0.29
	0.0289	389747	3.09e-2	0.66	6.47e-2	0.72	2.23e-4	1.41	3.45e-2	0.73	6.16e-0	-0.30
	0.0218	685491	2.56e-2	0.66	5.29e-2	0.71	1.51e-4	1.38	2.82e-2	0.72	6.70e-0	-0.30
2	0.1179	47809	5.01e-2	--	1.51e-1	--	7.06e-4	--	9.45e-2	--	3.81e-0	--
	0.0786	107353	3.82e-2	0.67	1.13e-1	0.72	3.96e-4	1.42	7.05e-2	0.72	4.29e-0	-0.29
	0.0429	360163	2.50e-2	0.70	7.12e-2	0.76	1.96e-4	1.16	4.43e-2	0.77	5.14e-0	-0.30
	0.0289	793507	1.96e-2	0.61	5.53e-2	0.64	1.01e-4	1.68	3.44e-2	0.64	5.77e-0	-0.29
	0.0218	1395811	1.63e-2	0.66	4.53e-2	0.70	6.74e-5	1.43	2.86e-2	0.65	6.28e-0	-0.30

Table 5.7: Example 3, history of convergence using triangles.

k	h	N	$e(t)$	$r(t)$	$e(\sigma)$	$r(\sigma)$	$e(u)$	$r(u)$	$e(p)$	$r(p)$	$e(\sigma^*)$	$r(\sigma^*)$
0	0.1512	3985	1.49e-1	--	3.65e-1	--	6.08e-2	--	2.06e-1	--	5.70e-0	--
	0.0825	13245	1.05e-1	0.58	2.12e-1	0.89	3.35e-2	0.99	1.05e-1	1.10	7.46e-0	-0.44
	0.0422	50268	6.85e-2	0.64	1.33e-1	0.70	1.71e-2	1.00	6.48e-2	0.73	9.88e-0	-0.42
	0.0283	111105	5.14e-2	0.72	9.76e-2	0.78	1.15e-2	1.00	4.72e-2	0.79	1.15e+1	-0.39
	0.0211	200381	4.21e-2	0.67	7.93e-2	0.70	8.58e-3	1.00	3.82e-2	0.72	1.28e+1	-0.36
1	0.1512	12721	2.79e-1	--	2.17e-0	--	6.58e-3	--	1.51e-0	--	6.44e-0	--
	0.0825	42461	1.89e-1	0.65	1.71e-0	0.39	2.94e-3	1.33	1.20e-0	0.38	8.24e-0	-0.41
	0.0422	161552	1.30e-1	0.56	1.24e-0	0.48	1.17e-3	1.37	8.70e-1	0.47	1.13e+1	-0.47
	0.0283	357377	1.00e-1	0.65	8.91e-1	0.84	6.48e-4	1.49	6.51e-1	0.73	1.31e+1	-0.38
	0.0211	644829	8.23e-2	0.67	7.21e-1	0.72	4.20e-4	1.46	5.30e-1	0.69	1.46e+1	-0.36
2	0.1512	25345	1.74e-1	--	6.08e-0	--	3.88e-3	--	4.29e-0	--	8.43e-0	--
	0.0825	84745	1.30e-1	0.48	3.87e-0	0.74	1.96e-3	1.13	2.74e-0	0.74	9.61e-0	-0.22
	0.0422	322759	8.04e-2	0.72	2.25e-0	0.81	8.95e-4	1.17	1.59e-0	0.81	1.21e+1	-0.35
	0.0283	714241	6.18e-2	0.66	1.65e-0	0.78	5.38e-4	1.28	1.18e-0	0.75	1.38e+1	-0.33
	0.0211	1288969	5.06e-2	0.67	1.33e-0	0.71	3.66e-4	1.31	9.66e-1	0.67	1.54e+1	-0.37

Table 5.8: Example 3, history of convergence using quadrilaterals.

k	h	N	$e(\mathbf{t})$	$r(\mathbf{t})$	$e(\boldsymbol{\sigma})$	$r(\boldsymbol{\sigma})$	$e(\mathbf{u})$	$r(\mathbf{u})$	$e(p)$	$r(p)$	$e(\boldsymbol{\sigma}^*)$	$r(\boldsymbol{\sigma}^*)$
0	0.0770	12708	2.03e-1	--	1.50e+1	--	3.92e-2	--	1.06e+1	--	1.68e+1	--
	0.0462	35038	1.27e-1	0.93	1.01e+1	0.79	2.30e-2	1.04	7.11e-0	0.79	1.90e+1	-0.24
	0.0330	68456	1.05e-1	0.55	8.35e-0	0.55	1.63e-2	1.03	5.83e-0	0.59	2.15e+1	-0.37
	0.0257	112962	8.99e-2	0.63	6.80e-0	0.82	1.25e-2	1.05	4.90e-0	0.69	2.35e+1	-0.35
	0.0204	178148	7.89e-2	0.57	5.73e-0	0.74	9.78e-3	1.06	4.08e-0	0.79	2.56e+1	-0.37
1	0.0770	38120	1.39e-1	--	1.42e+1	--	4.80e-3	--	1.00e+1	--	1.58e+1	--
	0.0462	105110	1.01e-1	0.63	9.33e-0	0.82	2.87e-3	1.01	6.81e-0	0.76	1.78e+1	-0.23
	0.0330	205364	8.10e-2	0.65	7.23e-0	0.76	1.53e-3	1.87	5.32e-0	0.74	2.09e+1	-0.49
	0.0257	338882	6.64e-2	0.79	6.12e-0	0.66	1.09e-3	1.34	4.32e-0	0.83	2.30e+1	-0.37
	0.0204	534440	5.68e-2	0.67	5.15e-0	0.75	8.14e-4	1.28	3.64e-0	0.74	2.51e+1	-0.38
2	0.0770	73927	1.61e-1	--	2.44e+1	--	5.00e-3	--	1.73e+1	--	2.35e+1	--
	0.0462	203847	1.12e-1	0.71	1.54e+1	0.91	2.39e-3	1.45	1.09e+1	0.91	2.73e+1	-0.29
	0.0330	398279	8.36e-2	0.87	1.24e+1	0.64	1.48e-3	1.43	8.77e-0	0.64	3.09e+1	-0.37
	0.0257	657223	6.92e-2	0.75	9.95e-0	0.88	1.04e-3	1.40	7.43e-0	0.66	3.39e+1	-0.36
	0.0204	1036487	5.96e-2	0.64	8.44e-0	0.72	7.81e-4	1.23	6.35e-0	0.68	3.66e+1	-0.34

Table 5.9: Example 3, history of convergence using hexagons.

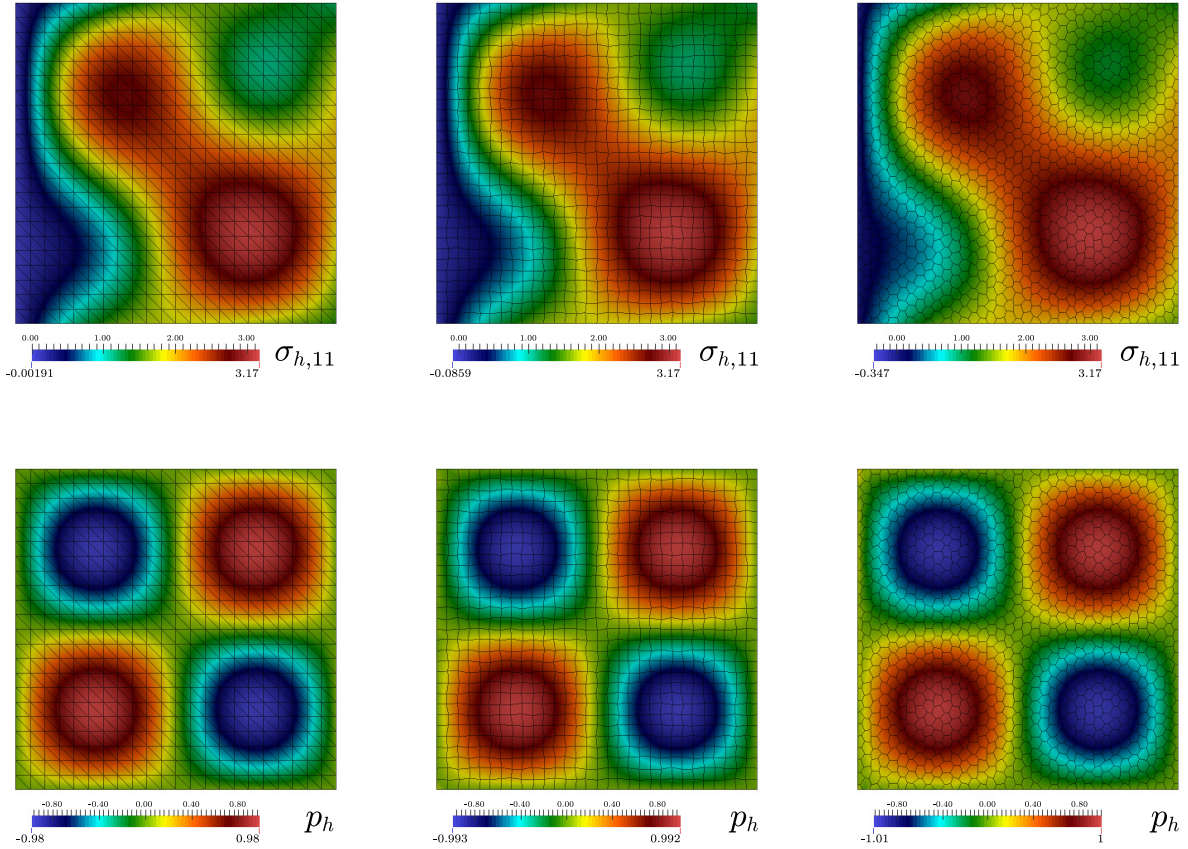


Figure 5.1: Example 2, $\sigma_{h,11}$ (top) and p_h (bottom).

References

- [1] B. AHMAD, A. ALSAEDI, F. BREZZI, L.D. MARINI AND A. RUSSO, *Equivalent projectors for virtual element methods*. *Comput. Math. Appl.* 66 (2013), no. 3, 376–391.
- [2] J. BARANGER, K. NAJIB AND D. SANDRI, *Numerical analysis of a three-fields model for a quasi-Newtonian flow*. *Comput. Methods Appl. Mech. Engrg.* 109 (1993), no. 3–4, 281–292.
- [3] L. BEIRÃO DA VEIGA, F. BREZZI, A. CANGIANI, L.D. MARINI, G. MANZINI AND A. RUSSO, *Basic principles of virtual elements methods*. *Math. Models Methods Appl. Sci.* 23 (2013), no. 1, 199–214.
- [4] L. BEIRÃO DA VEIGA, F. BREZZI AND L.D. MARINI, *Virtual elements for linear elasticity problems*. *SIAM J. Numer. Anal.* 51 (2013), no. 2, 794–812.
- [5] L. BEIRÃO DA VEIGA, F. BREZZI, L.D. MARINI AND A. RUSSO, *The hitchhiker guide to the virtual element method*. *Math. Models Methods Appl. Sci.* 24 (2014), no. 8, 1541–1573.
- [6] L. BEIRÃO DA VEIGA, F. BREZZI, L.D. MARINI AND A. RUSSO, *$H(\text{div})$ and $H(\text{curl})$ -conforming virtual element methods*. *Numer. Math.* 133 (2016), no. 2, 303–332.
- [7] L. BEIRÃO DA VEIGA, F. BREZZI, L.D. MARINI AND A. RUSSO, *Mixed virtual element methods for general second order elliptic problems on polygonal meshes*. *ESAIM Math. Model. Numer. Anal.* 50 (2016), no. 3, 727–747.
- [8] L. BEIRÃO DA VEIGA AND G. MANZINI, *A virtual element method with arbitrary regularity*. *IMA J. Numer. Anal.* 34 (2014), no. 2, 759–781.
- [9] F. BREZZI, R.S. FALK AND L.D. MARINI, *Basic principles of mixed virtual element methods*. *ESAIM Math. Model. Numer. Anal.* 48 (2014), no. 4, 1227–1240.
- [10] F. BREZZI AND M. FORTIN, *Mixed and Hybrid Finite Element Methods*. Springer-Verlag, 1991.
- [11] F. BREZZI AND L.D. MARINI, *Virtual element methods for plate bending problems*. *Comput. Methods Appl. Mech. Engrg.* 253 (2013), 455–462.
- [12] E. CÁCERES AND G.N. GATICA, *A mixed virtual element method for the pseudostress-velocity formulation of the Stokes problem*. *IMA J. Numer. Anal.* 37 (2017), no. 1, 296–331.
- [13] E. CÁCERES, G.N. GATICA AND F.A. SEQUEIRA, *A mixed virtual element method for the Brinkman problem*. *Math. Models Methods Appl. Sci.* DOI: 10.1142/S0218202517500142, to appear.
- [14] Z. CAI, CH. TONG, P.S. VASSILEVSKI AND CH. WANG, *Mixed finite element methods for incompressible flow: stationary Stokes equations*. *Numer. Methods Partial Differential Equations* 26 (2010), no. 4, 957–978.
- [15] V.J. ERVIN, J.S. HOWELL AND I. STANCULESCU, *A dual-mixed approximation method for a three-field model of a nonlinear generalized Stokes problem*. *Comput. Methods Appl. Mech. Engrg.* 197 (2008), no. 33–40, 2886–2900.
- [16] A.L. GAIN, C. TALISCHI AND G.H. PAULINO, *On the virtual element method for three-dimensional linear elasticity problems on arbitrary polyhedral meshes*. *Comput. Methods Appl. Mech. Engrg.* 282 (2014), no. 1, 132–160.

- [17] G.N. GATICA, L.F. GATICA AND A. MÁRQUEZ, *Analysis of a pseudostress-based mixed finite element method for the Brinkman model of porous media flow*. Numer. Math. 126 (2014), no. 4, 635–677.
- [18] G.N. GATICA, L.F. GATICA AND F.A. SEQUEIRA, *Analysis of an augmented pseudostress-based mixed formulation for a nonlinear Brinkman model of porous media flow*. Comput. Methods Appl. Mech. Engrg. 289 (2015), no. 1, 104–130.
- [19] G.N. GATICA, L.F. GATICA AND F.A. SEQUEIRA, *A $\mathbb{RT}_k - \mathbf{P}_k$ approximation for linear elasticity yielding a broken $\mathbb{H}(\mathbf{div})$ convergent postprocessed stress*. Appl. Math. Lett. 49 (2015), 133–140.
- [20] G.N. GATICA, L.F. GATICA AND F.A. SEQUEIRA, *A priori and a posteriori error analyses of a pseudostress-based mixed formulation for linear elasticity*. Comput. Math. Appl. 71 (2016), no. 2, 585–614.
- [21] G.N. GATICA, M. GONZÁLEZ AND S. MEDDAHI, *A low-order mixed finite element method for a class of quasi-Newtonian Stokes flows. I: A priori error analysis*. Comput. Methods Appl. Mech. Engrg. 193 (2004), no. 9-11, 881–892.
- [22] G.N. GATICA, A. MÁRQUEZ AND M.A. SÁNCHEZ, *Analysis of a velocity-pressure-pseudostress formulation for the stationary Stokes equations*. Comput. Methods Appl. Mech. Engrg. 199 (2010), no. 17-20, 1064–1079.
- [23] G.N. GATICA, A. MÁRQUEZ AND M.A. SÁNCHEZ, *A priori and a posteriori error analyses of a velocity-pseudostress formulation for a class of quasi-Newtonian Stokes flows*. Comput. Methods Appl. Mech. Engrg. 200 (2011), no. 17–20, 1619–1636.
- [24] G.N. GATICA AND F.A. SEQUEIRA, *Analysis of an augmented HDG method for a class of quasi-Newtonian Stokes flows*. J. Sci. Comput. 65 (2015), no. 3, 1270–1308.
- [25] J.S. HOWELL, *Dual-mixed finite element approximation of Stokes and nonlinear Stokes problems using trace-free velocity gradients*. J. Comput. Appl. Math. 231 (2009), no. 2, 780–792.
- [26] O. LADYZHENSKAYA, *New equations for the description of the viscous incompressible fluids and solvability in the large for the boundary value problems of them*. Boundary Value Problems of Mathematical Physics V, Providence, RI: AMS, 1970.
- [27] A.F.D. LOULA AND J.N.C. GUERREIRO, *Finite element analysis of nonlinear creeping flows*. Comput. Methods Appl. Mech. Engrg. 79 (1990), no. 1, 87–109.
- [28] D. MORA, G. RIVERA AND R. RODRÍGUEZ, *A virtual element method for the Steklov eigenvalue problem*. Math. Models Methods Appl. Sci. 25 (2015) 1421–1445.
- [29] D. SANDRI, *Sur l’approximation numérique des écoulements quasi-Newtoniens dont la viscosité suit la loi puissance ou la loi de Carreau*. Math. Model. Numer. Anal. 27 (1993), no. 2, 131–155.
- [30] B. SCHEURER, *Existence et approximation de points selles pour certains problèmes non linéaires*. RAIRO Anal. Numér. 11 (1977), no. 4, 369–400.